



5-2007

New Wings for the T-38: A Computational Performance Evaluation of the T-38 Aircraft with a New Wing Design

John M. Kanuch

University of Tennessee - Knoxville

Recommended Citation

Kanuch, John M., "New Wings for the T-38: A Computational Performance Evaluation of the T-38 Aircraft with a New Wing Design. " Master's Thesis, University of Tennessee, 2007.
https://trace.tennessee.edu/utk_gradthes/253

This Thesis is brought to you for free and open access by the Graduate School at Trace: Tennessee Research and Creative Exchange. It has been accepted for inclusion in Masters Theses by an authorized administrator of Trace: Tennessee Research and Creative Exchange. For more information, please contact trace@utk.edu.

To the Graduate Council:

I am submitting herewith a thesis written by John M. Kanuch entitled "New Wings for the T-38: A Computational Performance Evaluation of the T-38 Aircraft with a New Wing Design." I have examined the final electronic copy of this thesis for form and content and recommend that it be accepted in partial fulfillment of the requirements for the degree of Master of Science, with a major in Aviation Systems.

Stephen Corda, Major Professor

We have read this thesis and recommend its acceptance:

Frank G. Collins, UP Solies

Accepted for the Council:

Dixie L. Thompson

Vice Provost and Dean of the Graduate School

(Original signatures are on file with official student records.)

To the Graduate Council:

I am submitting herewith a thesis written by John M. Kanuch entitled “New Wings for the T-38: A Computational Performance Evaluation of the T-38 Aircraft with a New Wing Design.” I have examined the final electronic copy of this thesis for form and content and recommend that it be accepted in partial fulfillment of the requirements for the degree of Master of Science, with a major in Aviation Systems.

Stephen Corda
Dr. Stephen Corda, Major Professor

We have read this thesis
and recommend its acceptance:

Frank G. Collins

UP Solies

Accepted for the Council:

Carolyn Hodges

Vice Provost and Dean of the
Graduate School

(Official signatures are on file with official student records)

NEW WINGS FOR THE T-38:

**A COMPUTATIONAL PERFORMANCE EVALUATION OF THE T-38 AIRCRAFT
WITH A NEW WING DESIGN**

A Thesis
Presented for the
Master of Science
Degree
The University of Tennessee, Knoxville

John M. Kanuch
May 2007

DEDICATION

I wish to thank the members of my thesis committee from the University of Tennessee Space Institute: Dr. Stephen Corda, Dr. Peter Solies, and Dr. Frank Collins. Also, I would like to thank Mr. Reagan Woolf for sharing his computer programming skills and aircraft performance knowledge with me. Finally, thanks go to Mr. Frank Brown, for his technical expertise, guidance, and mentoring over the past three years of T-38 flight test.

Abstract

Despite the recent improvements to the T-38 airframe and engines, the United States Air Force is still seeking ways to improve the aircraft's takeoff, cruise, and landing performance. One potential way to improve the performance is to change the design of the wing. Using the Digital Performance Simulation aircraft-performance computer code, a T-38C performance evaluation sensitivity study was performed by parametrically varying the wing design. The computer model was a three degree of freedom, point-mass, batch simulation. The design changes investigated included varying aspect ratio with constant wing area, varying wing area with constant aspect ratio, and the addition of a winglet. These preliminary design estimates compared the differences in takeoff, cruise, and landing phases resulting from the modifications to the current baseline configuration. Using a variety of aerodynamic theories, new aircraft lift curves and drag polars were developed. These new aerodynamic models were then used in the computer simulation to determine the new aircraft performance during the various phases of flight. While incremental improvements were made in maximum range, maximum speed, and landing distances, a major improvement in the single-engine climb performance was found with a small increase in wing area from the baseline value of 170.0 square feet to 183.7 square feet. With a weight gain of only approximately 138 pounds, the operational envelope of the aircraft can be significantly increased. This larger wing will provide a 10 knot improvement in single engine takeoff speed and a 7.5% reduction in landing distance and will allow continued operation of the aircraft in the most demanding environmental conditions.

TABLE OF CONTENTS

	<u>Page Number</u>
INTRODUCTION	1
Background	1
Recent Aircraft Improvements	3
T-38C Avionics Upgrade Program (AUP).....	3
T-38C Propulsion Modernization Program (PMP).....	3
Aircraft Performance and Mission Issues	5
Performance Areas.....	5
Objectives.....	6
Overview	6
AERODYNAMIC AND PERFORMANCE THEORY	8
Assumptions	8
Atmosphere	8
Lift and Drag Curves	8
Wing Characteristics.....	8
Airframe Characteristics	9
Engine Characteristics.....	9
Mission Areas.....	9
Takeoff.....	9
Cruise	10
Maximum Range.....	10
Maximum Speed.....	11
Landing	11
Theory	11
Aspect Ratio Changes.....	12
Wing Reference Area Changes.....	12
Stall Speed.....	14
Addition of Winglets.....	16
ANALYSIS TECHNIQUE.....	18
Digital Performance Simulation (DPS)	18
Function.....	18
Data Requirements.....	18
Inputs.....	18
Outputs	18
Design Configuration Test Matrix.....	19
Aspect Ratio Changes	19
Selection Criteria	19
Wing Reference Area Changes.....	21
Selection Criteria	21
Addition of Winglets.....	23
Selection Criteria	23
Modification of the Lift Curves.....	23
Aspect Ratio Changes	23

Wing Reference Area Changes.....	23
Addition of Winglets.....	26
Modification of the Drag Polars.....	26
Aspect Ratio Changes.....	26
Wing Reference Area Changes.....	27
Addition of Winglets.....	27
Computer Data Procedures and Run Tables.....	28
Aspect Ratio Changes.....	28
Wing Reference Area Changes.....	28
Addition of Winglets.....	28
SETOS.....	32
Maximum Range.....	32
Maximum Speed.....	33
Minimum Speed.....	33
Error Analysis.....	34
RESULTS AND DISCUSSION.....	35
Takeoff.....	35
Aspect Ratio Results.....	35
Wing Area Results.....	35
Winglet Results.....	35
Cruise.....	39
Maximum Range.....	39
Aspect Ratio Results.....	39
Wing Area Results.....	41
Winglet Results.....	41
Maximum Speed.....	41
Aspect Ratio Results.....	46
Wing Area Results.....	46
Winglet Results.....	46
Landing.....	46
Stall Speed.....	46
Aspect Ratio Results.....	46
Wing Area Results.....	50
Winglet Results.....	50
Wing Weights.....	50
SUMMARY OF RESULTS.....	54
SETOS.....	54
Maximum Range.....	54
Maximum Speed.....	56
Landing Distances.....	56
CONCLUSIONS.....	57
REFERENCES.....	59
APPENDIX A.....	61
APPENDIX B.....	69
APPENDIX C.....	70

LIST OF ILLUSTRATIONS

Title	Page Number
Figure 1. T-38 Talon Supersonic Jet Trainer Aircraft.	2
Figure 2. T-38C cockpit after the Avionics Upgrade Program.	3
Figure 3. Comparison of non-modified (L) and modified (R) T-38 inlets.	4
Figure 4. Comparison of non-modified (L) and modified (R) T-38 nozzles.	4
Figure 5. Full span wing diagrams for aspect ratio variations.	20
Figure 6. Semi-span wing diagrams for aspect ratio variations.	20
Figure 7. Wing diagrams for wing area variations.	22
Figure 8. Wing diagrams for wing area variations.	22
Figure 9. Winglet design.	24
Figure 10. Lift coefficient versus angle of attack for Mach = 0.	25
Figure 11. Drag Polars for Mach = 0.	27
Figure 12. Aspect Ratio Analysis Flowchart	29
Figure 13. Reference Area Analysis Flowchart	30
Figure 14. Winglet Analysis Flowchart	31
Figure 15. SETOS iteration example.	33
Figure 16. SETOS trend versus aspect ratio.	36
Figure 17. SETOS trend versus wing area.	37
Figure 18. SETOS trend versus aspect ratio with winglet point added.	38
Figure 19. Specific range plots for variation in aspect ratio.	39
Figure 20. Maximum specific range variation with aspect ratio.	40
Figure 21. Specific range plots for variation in wing area.	42
Figure 22. Maximum specific range variation with wing area.	43
Figure 23. Specific range plots for baseline and winglet.	44
Figure 24. Maximum specific range with winglet.	45
Figure 25. Maximum speed profile for variations in aspect ratio.	47
Figure 26. Maximum speed profile for variations in wing area.	48
Figure 27. Maximum speed profile with winglet.	49
Figure C-1. Example of DPS input file for SETOS level acceleration	70
Figure C-2. Example of DPS input file for SETOS climb.	70
Figure C-3. Example of DPS input file for maximum range	70
Figure C-4. Example of DPS input file for maximum speed profile.	71

LIST OF TABLES

Title	Page Number
Table 1. T-38 Aircraft General Characteristics.....	2
Table 2. T-38 Wing Characteristics.....	6
Table 3. Critical Field Length temperatures and SETOS for various altitudes.	Error!
Bookmark not defined.	
Table 4. Critical Field Length temperatures and SETOS for various altitudes.	Error!
Bookmark not defined.	
Table 5. Wing parameters for variations in aspect ratio.....	19
Table 6. Wing parameters for variation in wing area.	21
Table 7. Comparison of baseline to winglet parameters.....	24
Table 8. Lift curve values for Mach = 0	25
Table 9. Lift coefficient and drag coefficient values for Mach = 0.....	26
Table 10. Aspect Ratio Run Matrix.....	29
Table 11. Wing Area Run Matrix.....	30
Table 12. Winglet Run Matrix	31
Table 13. SETOS values for varying aspect ratios.....	36
Table 14. SETOS values for varying wing areas.	37
Table 15. SETOS values for wing-winglet combination.....	38
Table 16. Variation of maximum specific range with aspect ratio.	40
Table 17. Variation of maximum specific range with wing area.	42
Table 18. Variation of maximum specific range with winglet added.	44
Table 19. Maximum Mach numbers for variation in aspect ratio.....	47
Table 20. Maximum Mach numbers for variation in wing area.....	48
Table 21. Maximum Mach number with winglet.....	49
Table 22. Effect of wing area changes on stall speed, landing speed, and landing distance for 12,500 lbs.	51
Table 23. Effect of wing area changes on stall speed, landing speed, and landing distance for 9,700 lbs.	51
Table 24. Weight of proposed wings for varying aspect ratio.	53
Table 25. Weight of proposed wings for varying wing areas.	53
Table 26. Summary of SETOS results.....	55
Table 27. Equivalent temperatures for baseline SETOS values.....	55
Table 28. Maximum range summary for a 2000 pound fuel burn.	55
Table 29. Maximum speed summary.....	56
Table 30. Landing distance summary.....	56

LIST OF ABBREVIATIONS, ACRONYMS, AND SYMBOLS

<u>Abbreviation</u>	<u>Definition</u>
α	Angle of Attack
a	Acceleration
ANG	US Air National Guard
AR	Aspect Ratio
A/S	Airspeed
AUP	Avionics Upgrade Program
b	Span
B	Baseline
C	Degrees Celsius
C_D	Drag Coefficient
C_{D_0}	Zero-lift Drag Coefficient
C_L	Lift Coefficient
c_{tip}	Wing-tip Chord Length
c_{root}	Wing-root Chord Length
CFL	Critical Field Length
d	Distance
D	Drag
D_i	Induced Drag
deg	Degrees
DPS	Digital Performance Simulation
e	Wing Efficiency Factor
F	Degrees Fahrenheit
ft	Feet
g	Acceleration Factor
GE	General Electrics
h	Winglet Height
KIAS	Knots Indicated Airspeed
L	Lift/Left
lb(s)	Pound(s)
L/D	Lift to Drag Ratio
MAC	Mean Aerodynamic Chord
min	Minute
NACA	National Advisory Committee for Aeronautics
NASA	National Aeronautics and Space Administration
nam	Nautical Air Miles
nd	Non-dimensional
PA	Pressure Altitude
PMP	Propulsion Modernization Program
P_s	Specific Excess Power
q	Dynamic Pressure
ρ	Density

LIST OF ABBREVIATIONS, ACRONYMS, AND SYMBOLS (con't)

<u>Abbreviation</u>	<u>Definition</u>
R	Right
REF	Reference
S	Wing Reference Area
SETOS	Single Engine Takeoff Speed
SM	Stall Margin
sq	Square
SR	Specific Range
UPT	Undergraduate Pilot Training
US	United States
USAF	United States Air Force
V	Velocity
w	Component Weight
W	Weight

INTRODUCTION

Background

The T-38A is a two-place, supersonic jet trainer aircraft (Figure 1, Reference 1) used by the United States Air Force (USAF) to conduct Undergraduate Pilot Training (UPT) as well as a variety of other training missions. It is currently flown by the US Navy, NASA, and several foreign countries.

The Talon was designed in the mid-1950's and was first manufactured in the early 1960's by the Northrop Corporation, Los Angeles, California. Some of the original aircraft design requirements were that the aircraft be capable of supersonic flight, demonstrate an endurance of approximately 90 minutes, have good flying characteristics, and be safe to fly. Since the aircraft was going to train thousands of students and be flown in excess of 40 hours per month, the T-38 needed to possess good flying qualities.

A key feature in producing an aircraft with the required flying characteristics is the design of the wing. This is especially true for supersonic jet aircraft where wing sweep is a critical performance and flying qualities design feature. Aircraft with greater wing sweep tend to have less desirable aerodynamics and require larger vertical and horizontal tails to counterbalance these characteristics. Therefore, to produce an aircraft with an inherently stable wing, a medium sweep angle was chosen for the T-38 wing.

In addition, one of the primary design constraints was that the airframe, without fuel or avionics, was to weight less than 5,000 pounds. This restriction was placed on the designers in order to keep the total "fly-away" cost of the aircraft at less than \$750,000.

Based on the original engineering studies, a 190-square-foot wing was desired. But, in order to meet the weight and cost requirements, the wing area was reduced and the T-38 of today has a 170-square-foot wing. Had the 190-square-foot wing been used, the whole airframe would have grown and caused the weight to exceed this 5,000-pound limit. The general characteristics of the T-38 are listed in Table 1 (Reference 2).



Figure 1. T-38 Talon Supersonic Jet Trainer Aircraft.

Table 1. T-38 Aircraft General Characteristics.

Primary Function	Advanced jet pilot trainer
Manufacturer	Northrop Corporation
Power Plant	2 x General Electric J85-GE-5 turbojet engine w/ afterburner
Thrust	2,050 lbf dry thrust, 2,900 lbf w/ afterburner
Thrust (with PMP)	2,200 lbf dry thrust, 3,300 lbf w/ afterburner
Weight	13,000 lbs (5900 kg) maximum takeoff weight
Length	46 feet, 4 inches (14 meters)
Height	12 feet, 10 inches (3.8 meters)
Wingspan	25 feet, 3 inches (7.6 meters)
Speed	812 mph (Mach 1.08 at sea level)
Ceiling	Above 55,000 feet (16,764 meters)
Range	1,093 miles
Armament	T-38A/C: none AT-38B: provisions for bomb dispenser
Unit Cost	\$756,000 (1961 constant dollars)
Crew	Two
Date Deployed	March 1961
USAF Inventory	Active force, 509; ANG, 0; Reserve 0

Recent Aircraft Improvements

T-38C Avionics Upgrade Program (AUP)

Beginning in 2000, the T-38 was modified with advanced avionics and all-glass cockpit displays to provide for more realistic flight training. The modifications to the front cockpit can be seen in Figure 2 (Reference 3).

These improvements to the 1960's cockpit allowed the student aircrew to learn about these advanced systems prior to encountering them in their follow-on fighter and bomber aircraft. This avionics upgrade program added approximately 300 pounds to the total weight of the aircraft.

T-38C Propulsion Modernization Program (PMP)

Based on a NASA study, the T-38 engine inlets and exhaust nozzles were modified as part of a propulsion modification program to improve the high-altitude, hot-weather performance of the aircraft. These changes can be seen in Figures 3 and 4 below (Reference 4).

In addition to the airframe changes, several components of the engine were updated to extend engine life. As a result of this program, the T-38 engines produced increased static thrust and reduced takeoff distance.



Figure 2. T-38C cockpit after the Avionics Upgrade Program.



Figure 3. Comparison of non-modified (L) and modified (R) T-38 inlets.

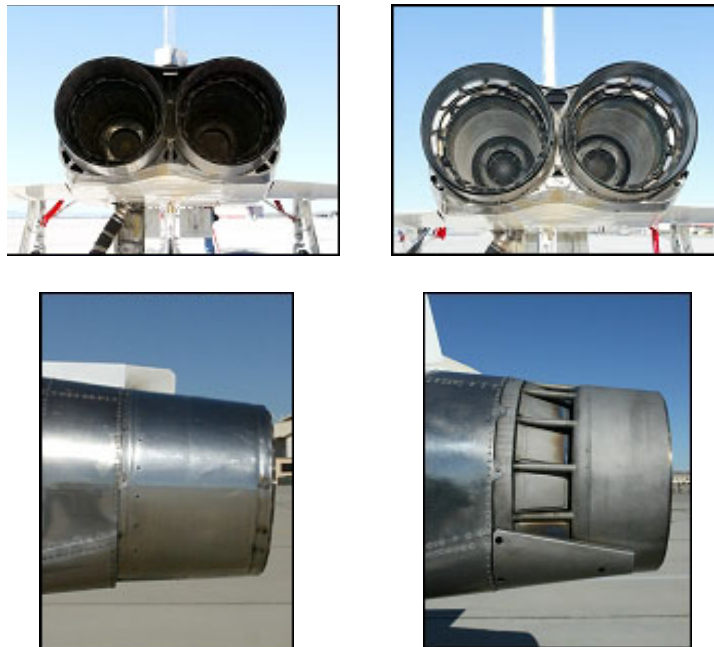


Figure 4. Comparison of non-modified (L) and modified (R) T-38 nozzles.

Aircraft Performance and Mission Issues

Most USAF T-38 bases are located in the southern portion of the United States. These geographic locations take advantage of relatively good, year-round flying weather. One disadvantage of these southern bases is high temperatures, exceeding 100 degrees F at some bases, during the summer. As temperature increases, the T-38 performance deteriorates, eventually reaching a point where a single-engine takeoff is no longer possible. T-38 flying is suspended at this point resulting in canceled sorties and missed student training deadlines.

In 2000, the USAF improved the performance of the T-38C by enlarging the inlets and modifying the nozzles. While the larger intake increased the total pressure of the airflow entering the engines and increased the static thrust, the larger intake created more spillage drag in flight. Although the hot weather performance was improved to a certain degree, the aircraft's overall performance improvement fell short of the desired goals.

Another area for possible improvement that was not investigated is the re-design of the aircraft's wing. The current T-38 wing characteristics are listed below in Table 2 (Reference 5).

There are several characteristics of the current wing that could be modified. First, due to the supersonic nature of the original aircraft design and no leading edge flaps, the thin, symmetric airfoil leads to high takeoff and landing speeds. These high speeds result in longer takeoff and landing distances. As the ambient temperature increases, the aircraft uses more and more of the available runway until, in the event of an engine failure, a single-engine takeoff is no longer possible.

Second, the wing has a simple hinged flap that results in smaller values of the maximum lift coefficient than is possible with the incorporation of other high lift devices. This affects takeoff and landing distances as well.

Thirdly, the thin wing limits the internal volume available for fuel or more complex flap designs. Finally, the small wing area and short aspect ratio lead to smaller lift coefficient values for a given angle of attack and higher values of induced drag.

Performance Areas

In order to understand the effects of wing modifications on the overall T-38 mission, the present study investigated representative maneuvers encountered during a typical flight. The performance areas analyzed were takeoff, cruise, and landing.

Table 2. T-38 Wing Characteristics

Airfoil	Modified NACA 65A004.8
Span	25.25 feet (7.70 m)
Reference Area	170.0 ft ² (15.8 m ²)
Root Cord	11.22 feet (3.42 m)
Tip Cord	2.24 feet (0.683 m)
Aspect Ratio	3.75
Taper Ratio	0.2
Span/Thickness Ratio	51.1
¼ Chord Sweep Angle	24 degrees
Dihedral Angle	0 degrees
Wing Incident Angle	0 degrees

Objectives

By using a computer simulation and utilizing actual lift, drag, and thrust models for the T-38C, the effects of the T-38 wing re-design were investigated. The analysis assessed the changes in performance of the T-38 by parametrically varying the wing design using three methods: 1) varying the aspect ratio while keeping the wing area constant, 2) varying the wing area while keeping the aspect ratio constant, and 3) investigating the addition of winglet design.

The primary objectives of this study were to evaluate the changes in T-38C performance for the following parametric variations in the wing design.

- 1) Wing aspect ratio
- 2) Wing planform area
- 3) Addition of a winglet

Overview

The present study used the Digital Performance Simulation (DPS) program (Reference 6) containing the T-38C aerodynamic and thrust models. DPS is a three degree of freedom, point-mass, FORTRAN computer program used to compute mission performance or point performance for a given aircraft. DPS is the standard program used to develop and analyze the current aerodynamic and thrust models for the T-38C. It contains flight test derived data collected and verified by the Air Force Flight Test Center at Edwards AFB,

California. The data used by DPS are the same data that are used to develop the flight manuals for the aircraft.

This study will vary the size and shape of the wing of the T-38. These changes in wing shape will be modeled using the various aerodynamic theories described below. The modified data for these models are then placed in the look-up tables used by DPS for the lift and drag coefficients. All lift and drag coefficient values used by DPS and referenced in this study are whole-aircraft and derived from flight test. The angle of attack values are from the fuselage reference line and are absolute angles of attack.

Optimum area-ruling of the aircraft fuselage was assumed in this analysis. If the aircraft wing were to be modified, then the new area-rule variations would need to be calculated causing substantial changes to the aircraft structure.

AERODYNAMIC AND PERFORMANCE THEORY

Assumptions

Atmosphere

The temperatures and pressures altitudes used were from the 1976 U.S. Standard Atmosphere (Reference 7). Key points to be noted are that the standard temperature at 4,000 feet pressure altitude is 7.1 degrees C (44.7 degrees F), decreases linearly until approximately 36,000 feet, and is then constant to altitudes exceeding 50,000 feet.

Lift and Drag Curves

Only out of ground-effect lift and drag curves were analyzed. No in-ground effect curves were analyzed. It was assumed that any performance changes out of ground effect would also be seen in ground effect.

Wing Characteristics

Leading edge sweep and taper ratio were assumed constant for all proposed wing designs. The baseline wing has a 24 degree wing sweep angle at the 25% mean aerodynamic chord (MAC) and a taper ratio of 0.2. From Reference 8, this combination closely approximates an elliptical lift distribution over the entire span.

Varying either the wing sweep angle or the taper ratio would lead to significant performance changes and therefore, both were held constant.

For increases in aspect ratio at a constant wing area, as span was increased, root and tip chords were reduced and trailing edge angle was also reduced to produce the desired aspect ratios. As previously mentioned, taper ratio remained at the baseline value of 0.2.

When aerodynamic reference area, S_{REF} , was varied, AR was held constant. For these cases, as span increased, both root chord and tip chord lengths were also increased. Since the leading edge sweep was being held constant, this meant that the increase in area for a constant aspect ratio was the result of a corresponding increase in root chord length. Again, taper ratio remained at a constant value of 0.2.

For many of the new wing geometries, the wing would still be able to be physically attached to the current structure of the airframe. This study was meant to provide a realistic look at possible wing changes that could be used on the current aircraft. In order to bound the problem, several configurations were studied that may not be able to be attached to the current airframe without seriously affecting other characteristics of the aircraft, e.g. center of gravity, handling qualities, weight and balance, structure, etc.

Airframe Characteristics

Optimum area-ruling was assumed in this analysis. This allowed direct comparison for supersonic portions of the analysis. However, the exact geometries were not determined in this study. If an aircraft were to be modified, then area rule variations would need to be calculated as the wing area was varied.

The computer model used the modified inlets and exhaust nozzles (see Figures 3 and 4) found on all PMP T-38C aircraft. These were not modified in the present study.

Engine Characteristics

The thrust model remained constant throughout the present study and equal to the baseline value. Installed thrust angle was constant and equal to the baseline value of 0.50 degrees nose up.

The engine model was not degraded. Therefore, the performance values calculated in this study by the computer model were greater than those listed in the T-38C flight manuals, since the T-38C flight manual is based on 98% of the thrust model and 105% of the fuel flow model.

Mission Areas

The three mission areas analyzed were takeoff, cruise, and landing. These represent performance critical areas of the T-38 flight envelope and also limit the present analyses to a manageable scope.

Takeoff

Due to the lightweight nature of the aircraft and the relatively high-thrust engines, the two-engine takeoff distances are well within the safety margins of the runways. For this reason, normal, two-engine takeoff distance was not analyzed. The key parameter of interest for the takeoff phase in the present study was single-engine takeoff speed (SETOS).

The definition of SETOS is the speed to which the aircraft must accelerate using a single engine (one engine in maximum power, the other off and windmilling) in order to obtain a 100 ft/min climb rate out of ground effect in the takeoff configuration (landing gear extended and flaps 60%).

SETOS imposes operational limitations on the aircraft. SETOS is closely related to critical field length (CFL). Once CFL is within 1000' of actual runway length, USAF T-38 aircraft are not allowed to conduct operations. For a 13,000 pound T-38 without PMP on a standard 8,000 foot runway for example, the ambient temperatures which cause CFL to equal 7,000 feet and the corresponding SETOS values are listed in Table 3 for altitudes

Table 3. Critical Field Length temperatures and SETOS for various altitudes. (7,000 CFL, Non-PMP)

Pressure Altitude (feet)	Temperature (C)	Temperature (F)	SETOS (KIAS)
0	18	64	171
1000	11	52	171
2000	3	37	170
4000	-18	0	170

Table 4. Critical Field Length temperatures and SETOS for various altitudes. (7,000 CFL, PMP)

Pressure Altitude (feet)	Temperature (C)	Temperature (F)	SETOS (KIAS)
0	36	97	179
1000	30	86	179
2000	24	75	179
4000	1	34	179

of sea level, 1000, 2000 and 4000 feet (Reference 9). The same T-38 with PMP values are listed in Table 4 (Reference 10). Increasing the takeoff performance of the aircraft will decrease both SETOS and CFL and allow operations at higher temperatures or similarly, higher pressure altitudes.

Due to limited aerodynamic data in the computer model, the normal SETOS aircraft configuration (landing gear extended and 60 degree flaps) could not be fully modeled in the present study. As a result, the gear retracted, 60% flaps extended configuration was selected and used during the data runs. Although the exact numerical values for the different airspeeds will not be identical, it is assumed that the observed trends with the gear retracted will be similar to those with the gear extended. SETOS was determined by calculating the airspeed that yields a specific excess power of 100 feet per minute for the various wing configurations.

Cruise

Maximum Range

To evaluate the changes in cruise performance, the maximum specific range of each wing configuration was determined. To be operationally representative, a typical T-38C cruise

altitude of 30,000 feet and a mission weight of 10,000 lbs were used in the simulation. The 10,000 lbs weight was representative of the end of a navigation mission.

Maximum Speed

The maximum speed in level, unaccelerated flight was calculated by determining the point at which the specific excess power was zero. At this point, the excess thrust of the system would also be zero. Maximum speeds were calculated for multiple altitudes for comparison between the various wing configurations.

This area of the analysis addressed the issue of whether the T-38 could still be a “supersonic” trainer. The baseline T-38 supersonic performance has been affected by the changes to the airframe (inlets and nozzles) and reductions in total thrust (degradation of the engines over time and detuning to extend core life). The current T-38 baseline performance is just over the Mach for a level acceleration, approximately Mach 1.07, well below the original design speed of approximately Mach 1.4.

Landing

The baseline T-38C stall speeds, for the gear extended and flaps 60% and 100% configurations, were compared to the current operational landing speeds to determine the operationally representative landing speed stall margin. Then, the theoretical new stall speeds for each new wing area were calculated and converted to the new landing speeds by keeping the same stall margins. Since landing distance is proportional to the square of landing speed, comparisons were made.

Maximum lift coefficient is the primary variable for stall speed. The wing camber and basic airfoil shape were not modified in the present study; therefore maximum lift coefficient was only affected by changes in the wing reference area.

Theory

The contributions of induced drag and form drag (parasite drag, skin friction drag, and interference drag) to the total drag are dependent on airspeed. As expected, at lower airspeeds, induced drag (drag due to lift) is the largest component of the total drag. As the airspeed increases, form drag dominates. All of the methods used in this study primarily affect the induced drag at a given angle of attack. It will be shown that the greatest effects on the T-38 performance of the various wing changes will be realized in the lower airspeed phases of flight.

Baseline aerodynamic lift and drag curves were modified for changes in either aspect ratio, wing reference area, or the addition of winglets by using several theories. These modified values were used in the computer simulation to yield the new performance of the aircraft. Using this data, comparisons were made to the baseline configuration.

Aspect Ratio Changes

The Lanchester-Prandtl wing theory (Reference 11) was used to compare various wing aspect ratios. This theory holds for wings with elliptical spanwise distributions of lift. For constant lift coefficients, the drag coefficients (C_D) and angle of attack (α) of various aspect ratios can be related by the following equations.

$$C'_D = C_D + \frac{C_L^2}{\pi} \left(\frac{1}{AR'} - \frac{1}{AR} \right) \quad (1)$$

and

$$\alpha' = \alpha + \frac{C_L}{\pi} \left(\frac{1}{AR'} - \frac{1}{AR} \right) \quad (2)$$

where AR is the baseline aspect ratio and AR' is the new aspect ratio. Similarly, C_D is the baseline drag coefficient, C'_D is the new value. Finally, α is the baseline angle of attack and α' is the modified value.

The lift curves and drag polars for the T-38C aerodynamic model were contained in look-up tables (as attached files to the DPS program) of lift coefficient versus angle of attack and drag coefficient versus lift coefficient. The values for angle of attack at a given lift coefficient were recalculated for the various aspect ratios. Similarly, the drag coefficient values for a given lift coefficient were recalculated for the new aspect ratio. These new tables were then used in the computer simulation as the modified aerodynamic model for the new wing design. These calculations were performed for both the clean aircraft (gear and flaps retracted) lift and drag curves and for the 60% flap configuration (gear retracted, flaps 60%).

Wing Reference Area Changes

For changing wing reference area, a different approach was used. It was assumed that the non-lift dependent drag (fuselage and parasite) remains constant if referenced to the baseline wing area, S_{REF} .

$$D - D_i = C_{D_o} q S_{REF} \quad (3)$$

For the clean aircraft, the induced drag coefficient will not change for a given lift coefficient and wing aspect ratio if both are referenced to the true wing area S_{REF} .

$$C'_L = C_{L_{REF}} \left(\frac{S_{REF}}{S'} \right) \quad (4)$$

where C_L' is the new lift coefficient for the new wing area S' .

Rearranging,

$$C_{L_{REF}} = C_L' \left(\frac{S'}{S_{REF}} \right) \quad (5)$$

In general,

$$L = C_L q S \quad (6)$$

So, multiplying equation (6) by $\left(\frac{S_{REF}}{S_{REF}} \right)$,

$$L = C_L' S' q = C_L' \left(\frac{S'}{S_{REF}} \right) q S_{REF} \quad (7)$$

Substituting for $C_L' \left(\frac{S'}{S_{REF}} \right)$ yields,

$$L = C_{L_{REF}} q S_{REF} \quad (8)$$

Therefore, the required lift, L , is the same for a given test condition.

Similarly for induced drag at the new lift coefficient,

$$C_{D_i}' = \frac{(C_L')^2}{(\pi A Re)} \quad (9)$$

and,

$$D_i' = \frac{(C_L')^2}{(\pi A Re)} q S' \quad (10)$$

and substituting for C_L' ,

$$C_{D_i,REF} = \frac{\left[C_{L,REF} \left(\frac{S_{REF}}{S'} \right) \right]^2}{(\pi A Re)} \quad (11)$$

Finally,

$$D_i' = \frac{\left[C_{L,REF} \left(\frac{S_{REF}}{S'} \right) \right]^2}{(\pi A Re)} q S_{REF} = \frac{\left[C_{L,REF} \left(\frac{b_{REF}^2}{b'^2} \right) \right]^2}{(\pi A Re)} q S_{REF} \quad (12)$$

As equation 12 shows, for a constant aspect ratio, the reduction in induced drag is due to the increase in the span of the wing. In addition, the value of D_i' can be calculated using the baseline lift coefficient values and scaling the output by $\left(\frac{S_{REF}}{S'} \right)$.

The computer program was modified to calculate the values for the set of new wing areas. The baseline lift curves and induced drag curves were used. Since the lift required was the same for each condition, lift coefficient was the same. Therefore, the only change to the code was to multiply the lift coefficient used in the induced drag calculations by $\left(\frac{S_{REF}}{S'} \right)$.

The program used both the baseline parasite drag curves and skin friction drag curves for all configurations since these were not affected by a change in wing area.

Stall Speed

To determine the effect of wing planform area on stall speed, the following relationship was used.

For level flight,

$$W = L = \frac{\rho}{2} V^2 S_{REF} C_L \quad (13)$$

At stall,

$$W = L = \frac{\rho}{2} V_{STALL_REF}^2 S_{REF} C_{L_MAX} \quad (14)$$

Rearranging,

$$V_{STALL_REF}^2 = \frac{2W}{\rho S_{REF} C_{L_MAX}} \quad (15)$$

Setting up a ratio for the new wing area to the reference area yields,

$$\frac{(V'_{STALL})^2}{(V_{STALL_REF})^2} = \frac{\frac{2W}{(\rho S' C'_{L_MAX})}}{\frac{2W}{(\rho S_{REF} C_{L_MAX})}} \quad (16)$$

And, since weight and flight conditions for each case are the same, this reduces to,

$$\frac{(V'_{STALL})^2}{(V_{STALL_REF})^2} = \left(\frac{S'}{S_{REF}} \right) \left(\frac{C'_{L_MAX}}{C_{L_MAX}} \right) \quad (17)$$

Now, if higher order effects on maximum lift coefficient are ignored, the maximum lift coefficients are also the same, and this simplifies to

$$V'_{STALL} = V_{STALL_REF} \sqrt{\left(\frac{S_{REF}}{S'} \right)} \quad (18)$$

From Reference 12, ground-roll distance during landing can be calculated as follows:

$$d_{groundroll} = \frac{1}{2a} V_{LDG}^2 \quad (19)$$

where a is the deceleration of the aircraft and is a function of the total stopping force (rolling friction, drag, braking action, etc) and V_{LDG} is the touchdown speed of the aircraft.

So, with a held constant across the various wing changes, it can be assumed that landing distance is only proportional to the square of the landing speed.

$$d_{ldg} \approx V_{LDG}^2 \quad (20)$$

But, landing speed depends on stall margin (SM):

$$V_{LDG} = (SM)V_{STALL} \quad (21)$$

So,

$$d_{LDG} \approx ([SM]V_{STALL})^2 \quad (22)$$

Again, setting up a ratio for the new wing area to the reference area and assuming that stall margin remains constant yields

$$d'_{LDG} \approx d_{LDG_{REF}} \left(\frac{V'_{LDG}}{V_{LDG_{REF}}} \right)^2 \quad (23)$$

This reduces to,

$$d'_{LDG} \approx d_{LDG_{REF}} \left(\frac{S_{REF}}{S'} \right) \quad (24)$$

Addition of Winglets

Winglets reduce the induced drag of a wing by interacting with the wingtip vortices. A properly designed winglet is cambered and twisted in such a manner that the wingtip vortex flows creates a lift force on the winglet that has a forward component. This forward component acts counter to drag and reduces the overall wing drag (Reference 8).

Since the winglets do not contribute to the total lift produced by the wing, lift was calculated for a given wing using the baseline span length. In order to model the drag reduction, total drag was calculated using the effective span of the wing, which is defined as the baseline span plus the height of the winglets. As with the changes in aspect ratio, these curves were modified using the Lanchester-Prandtl equations (equations 1 and 2). For both the wing only and wing-winglet combination, the reference area is equal to the baseline value as the area of the winglet is assumed to be zero for the purpose of this study.

For subsonic Mach numbers,

$$C_{L_{WINGLET}} = C_{L_{BASELINE}} \quad (25)$$

and,

$$C_{D_{WINGLET}} = C_{D_{BASELINE}} + \frac{C_{L_{BASELINE}}^2}{\pi} \left(\frac{1}{AR_{EFFECTIVE}} - \frac{1}{AR_{BASELINE}} \right) \quad (26)$$

From Reference 13, for supersonic Mach numbers, it is assumed that the lift coefficient of the wing and winglet combination is the same as that of the baseline wing alone:

$$C_{L_{WINGLET}} = C_{L_{BASELINE}} \quad (27)$$

and for lift coefficients greater than 0.2,

$$C_{D_{WINGLET}} = C_{D_{BASELINE}} \quad (28)$$

and for lift coefficient less than 0.2 the drag coefficients are defined as,

$$C_{D_{WINGLET}} = (0.9)C_{D_{BASELINE}} \quad (29)$$

These drag formulas model the slight reduction in drag observed in Reference 13 at low lift coefficients during supersonic flight.

ANALYSIS TECHNIQUE

Digital Performance Simulation (DPS)

The present study used the T-38C aerodynamic and thrust models in the DPS program (Reference 6). DPS is a FORTRAN computer program used to compute mission performance or point performance for a given aircraft.

Function

DPS uses a three degree of freedom point-mass simulation. Using selected, pre-programmed “maneuvers”, e.g. climb/descent, acceleration/deceleration, pull-up, cruise, thrust limited turn, lift limited turn, terrain following, maximum speed, or specific excess power contours, various starting and ending parameters determine performance based on user-supplied inputs.

Data Requirements

Baseline lift coefficients and drag coefficients are in DPS data files (see Appendices A and B). The values are moved to a Microsoft Excel file in a spreadsheet format. The tables are then changed, based on theory, to new values. These new values were then used to create new data files, reformatted in the proper form, used in place of the originals data files, and subsequently referenced by the simulation. For each wing configuration (aspect ratio change, wing area change, or winglet), separate files were created.

Inputs

Required data inputs were the aerodynamic lift and drag models. These models contain the lift and drag coefficients for the operational envelope of the T-38. All other models in the program (e.g. maximum lift coefficients and the thrust model) were not modified by this study. In addition, each DPS maneuver had required starting and ending parameters. For each run, the value of each of these parameters was selected to achieve the desired data.

Outputs

The output from DPS was in tabular form with variables displayed depending on the type of maneuver performed. These tables were converted to Microsoft Excel files, plotted, and analyzed.

Design Configuration Test Matrix

Aspect Ratio Changes

The baseline aspect ratio (AR) for the T-38C is 3.75. For the present study, the span of the aircraft was increased in one-foot increments while holding the wing reference area, leading edge sweep angle, and taper ratio constant. This method was used for wing configurations AR-1 through AR-6. For configurations AR-7 and AR-8, the aspect ratio was selected first and then the span was calculated based on the wing reference area of 170.0 square feet. The aspect ratio therefore varied from a minimum value of 1.0 to a maximum value of 10.0 as listed in Table 5. This table also lists the root and tip cord lengths.

Selection Criteria

Varying only aspect ratio and keeping S_{REF} constant allowed a direct comparison of aerodynamic performance. All aerodynamic coefficients were referenced to the baseline wing area. By not changing this value, it was easier to isolate the effects of aspect ratio changes. Based on finite wing theory, the effects of increases in aspect ratio become less pronounced as the aspect ratio increases. Therefore, this analysis varied aspect ratio from 3.75 (baseline) to approximately 5.75. To confirm this, an aspect ratio of 10.0 was used to provide an upper bound. Similarly, an aspect ratio of 1.00 was used to bound the changes at the low aspect ratio extreme.

The full span and semi-span wings are shown in Figures 5 and 6, respectively.

Table 5. Wing parameters for variations in aspect ratio.

Wing Configuration	AR (nd)	S (sq ft)	$\frac{AR}{AR_{REF}}$	b (ft)	c_{root} (ft)	c_{tip} (ft)
Baseline	3.75	170.0	1.000	25.25	11.22	2.24
AR-1	4.05	170.0	1.081	26.25	10.79	2.16
AR-2	4.37	170.0	1.165	27.25	10.40	2.08
AR-3	4.69	170.0	1.252	28.25	10.03	2.01
AR-4	5.03	170.0	1.342	29.25	9.69	1.94
AR-5	5.38	170.0	1.435	30.25	9.37	1.87
AR-6	5.74	170.0	1.532	31.25	9.07	1.81
AR-7	1.00	170.0	0.267	13.04	21.73	4.35
AR-8	10.00	170.0	2.667	41.23	6.87	1.37

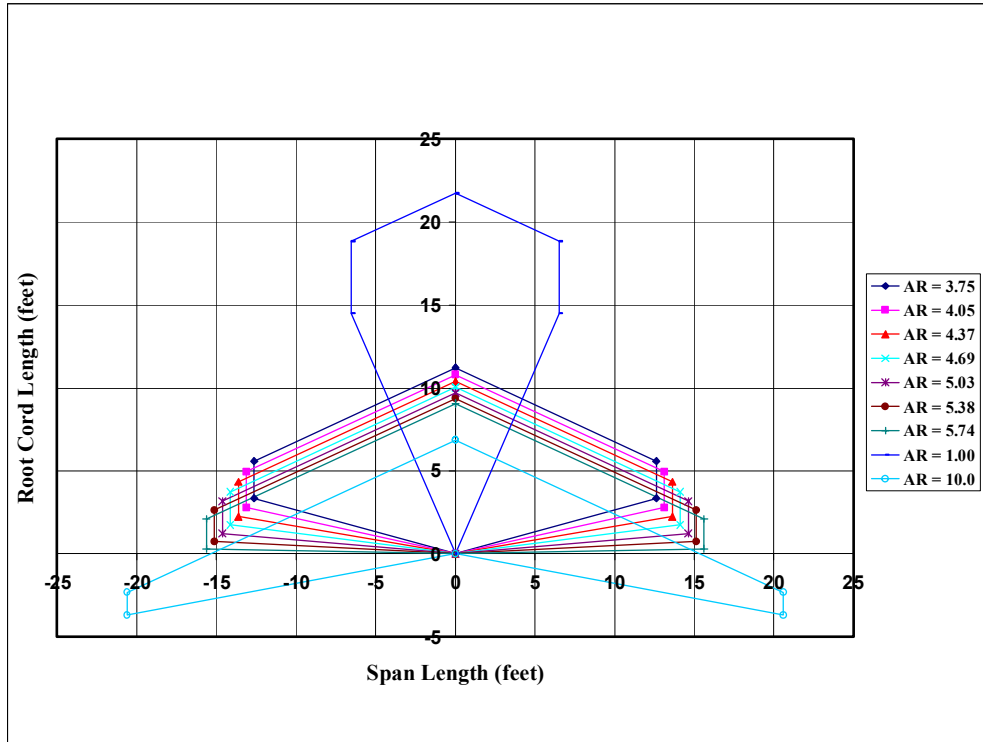


Figure 5. Full span wing diagrams for aspect ratio variations.

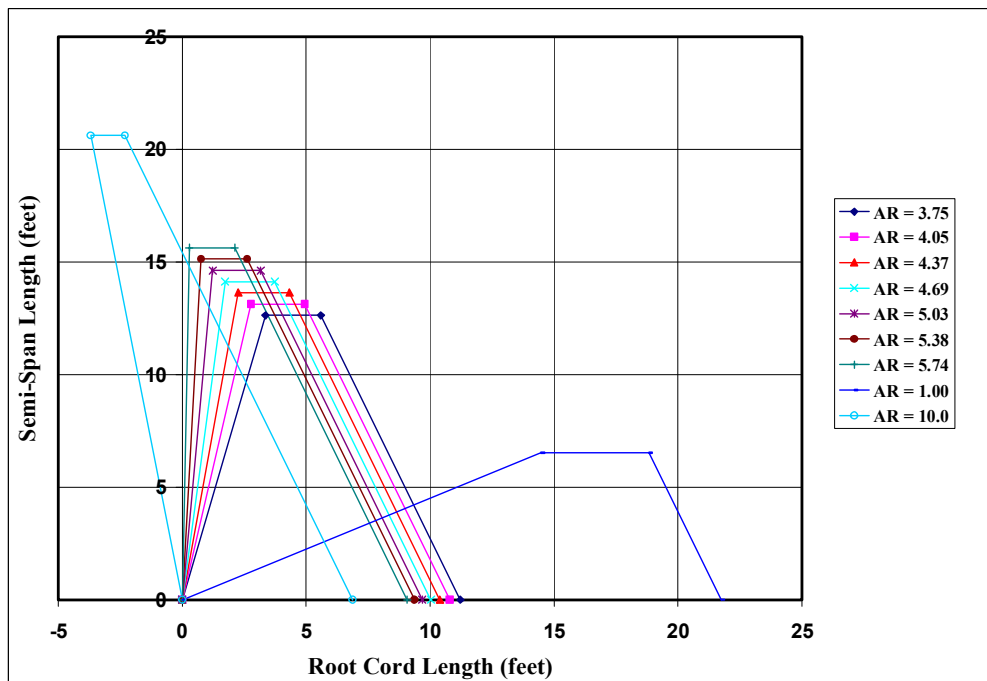


Figure 6. Semi-span wing diagrams for aspect ratio variations.

Wing Reference Area Changes

The baseline wing reference area (S_{REF}) for the T-38C is 170.0 square feet. For the present study, the wing span was increased in one-foot increments while holding the aspect ratio, leading edge sweep angle, and taper ratio constant. This method was used for wing configurations S-1 through S-6.

The wing area therefore varied from a minimum value of 170.0 square feet to a maximum value of 260.4 square feet as listed in Table 6.

The wing configurations created by varying the wing reference area are shown in Figure 7.

For clarity, the semi-span wing diagrams are depicted in Figure 8.

Selection Criteria

As previously discussed, these configurations required modification to the basic DPS code. The baseline aerodynamic lift and drag curves were not individually modified, but various outputs were scaled by the ratio of new wing area to reference area.

Table 6. Wing parameters for variation in wing area.

Wing Configuration	AR	S (sq ft)	$\frac{S}{S_{REF}}$	b (ft)	c_{root} (ft)	c_{tip} (ft)
Baseline	3.75	170.0	1.000	25.25	11.22	2.24
S-1	3.75	183.7	1.081	26.25	11.67	2.33
S-2	3.75	198.0	1.165	27.25	12.11	2.42
S-3	3.75	212.8	1.252	28.25	12.55	2.51
S-4	3.75	228.1	1.342	29.25	13.00	2.60
S-5	3.75	244.0	1.435	30.25	13.44	2.69
S-6	3.75	260.4	1.532	31.25	13.89	2.78

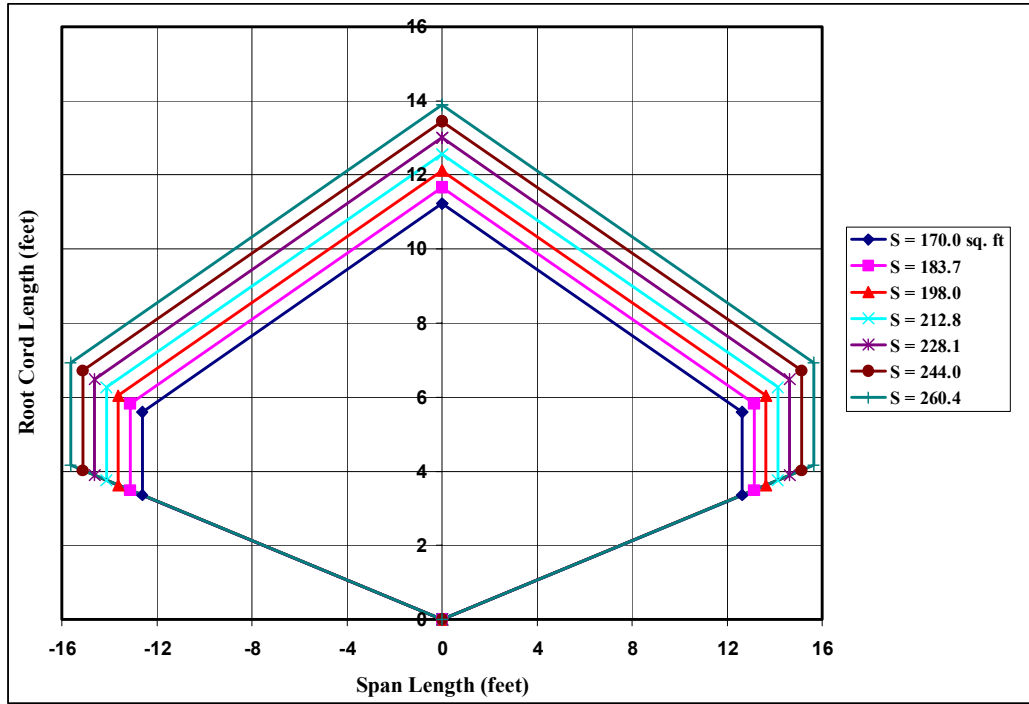


Figure 7. Wing diagrams for wing area variations.

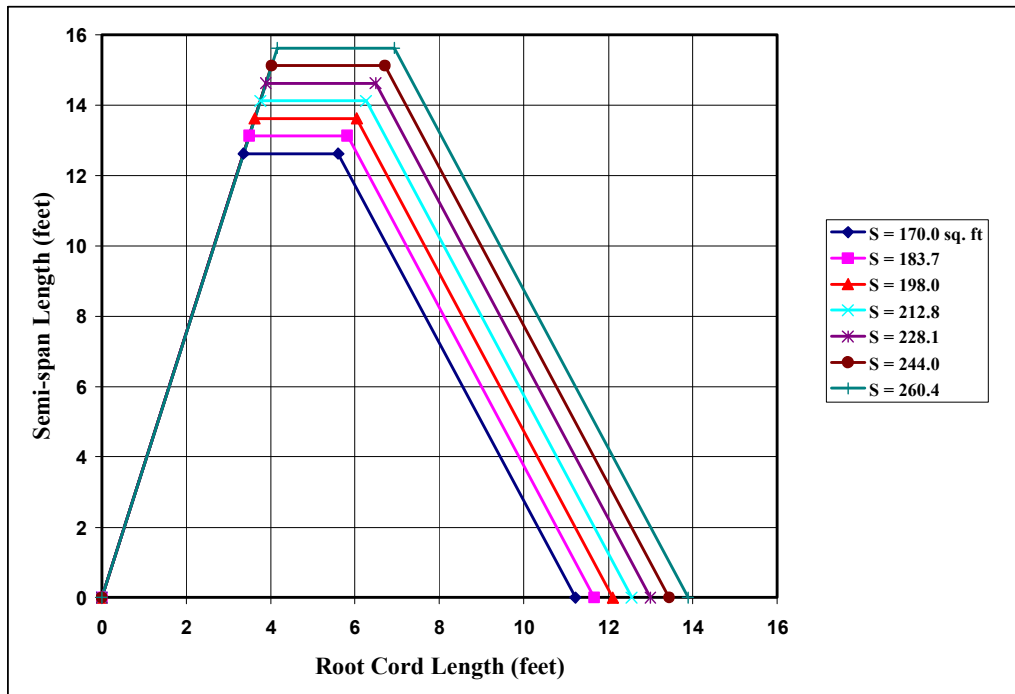


Figure 8. Wing diagrams for wing area variations.

Addition of Winglets

Only a single theoretical winglet design was studied. For the baseline span (b), the semi-span value ($b/2$) was multiplied by 15%, yielding the winglet height (h) used in Table 7 below. The effective aspect ratio is then used as described above. This wing and winglet combination is pictured in Figure 9.

Selection Criteria

As previously discussed, winglets decrease the induced drag of the wing at a given angle of attack. Using the 15% value for the height of the winglets allows the data from Reference 13 to be used for the supersonic study. The $AR_{\text{WINGLET}} / AR_{\text{BASELINE}}$ value of 1.32 was used to calculate the induced drag of the wing and winglet combination. This agrees with the $AR_{\text{WINGLET}} / AR_{\text{BASELINE}}$ value of 1.2 found in Reference 8. An in-depth study of the optimal winglet shape (toe angle, thickness ratios, taper ratios, sweep back angle, etc) is beyond the scope of this analysis, but the performance of the wing-winglet combination is illustrative of the potential of this configuration.

Modification of the Lift Curves

Aspect Ratio Changes

From the files contained in DPS of the aircraft lift coefficients and angle of attack data, Excel spreadsheet data files were created. These files contained the aerodynamic model over the Mach range of 0.0 to 1.6. For each aspect ratio configuration AR-1 through AR-8, the values were converted to the new values using the Lanchester-Prandtl equations (equations 1 and 2). This procedure was used for both the clean (landing gear retracted and wing flaps 0%) and the modified SETOS configuration (landing gear retracted and wing flaps 60%). An example for the Mach equal to zero case is illustrated in Table 8.

For the case of Mach equal to zero, each of these lift coefficient versus angle of attack tables was plotted (Figure 10). It can be confirmed that the progression of the modified curves with respect to changes in aspect ratio agrees with theory.

Wing Reference Area Changes

For all modified wing reference areas, the baseline lift coefficient and angle of attack data were used. No modification to the values of used in the aerodynamic model used by DPS was needed.

Table 7. Comparison of baseline to winglet parameters.

Winglet Configuration	AR	b (ft)	h (ft)	c_{root} (ft)	c_{tip} (ft)	S (sq ft)	$\frac{AR}{AR_{REF}}$
Baseline	3.75	25.25	0.00	11.22	2.24	170.0	1.00
W-1	4.96	25.25	1.89	11.22	2.24	170.0	1.32

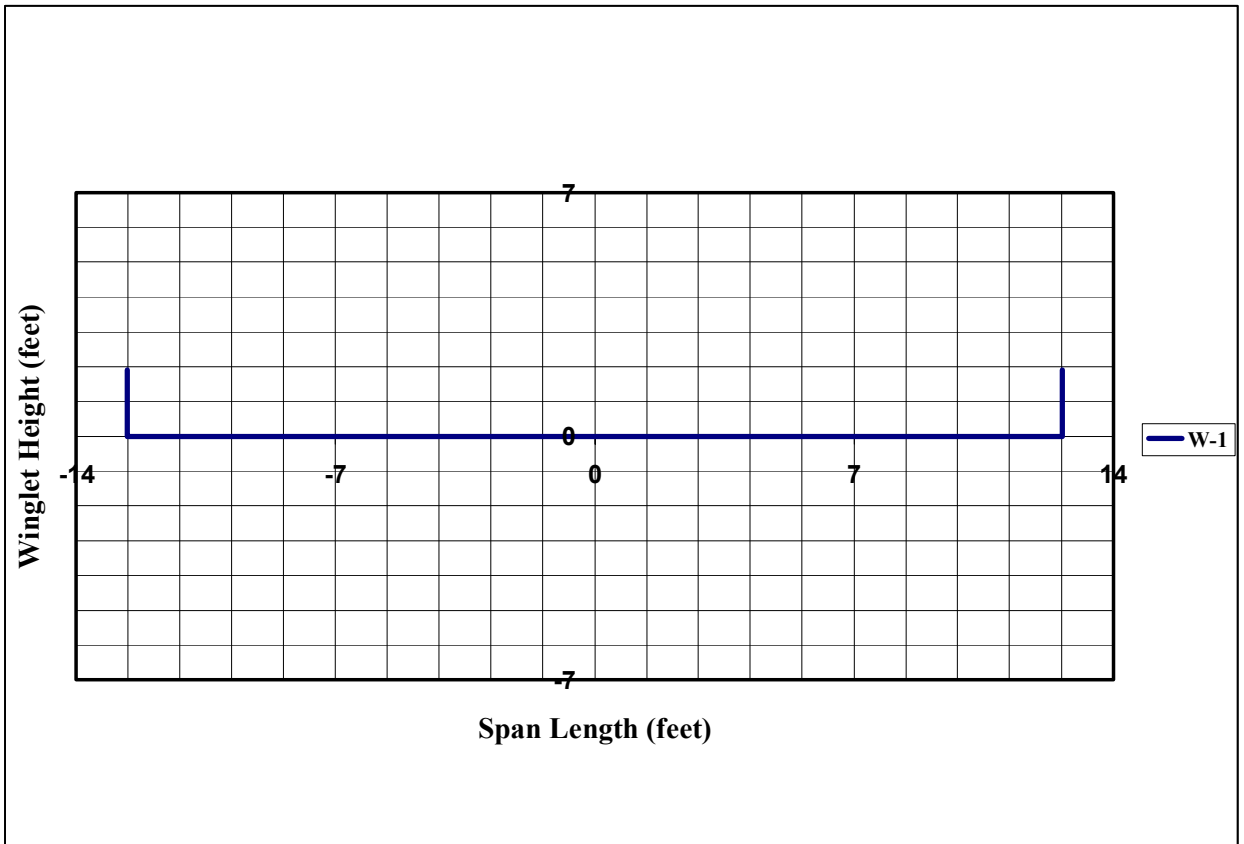


Figure 9. Winglet design.

Table 8. Lift curve values for Mach = 0

	Baseline	AR-1	AR-2	AR-3	AR-4	AR-5	AR-6	AR-7	AR-8
C_L	α (deg)	α (deg)	α (deg)	α (deg)	α (deg)	α (deg)	α (deg)	α (deg)	α (deg)
0.00	-0.033	-0.033	-0.033	-0.033	-0.033	-0.033	-0.033	-0.033	-0.033
0.10	1.447	1.410	1.378	1.349	1.323	1.299	1.278	2.784	1.143
0.20	2.926	2.853	2.789	2.730	2.678	2.631	2.588	5.601	2.318
0.30	4.405	4.296	4.199	4.112	4.034	3.963	3.899	8.418	3.494
0.40	5.885	5.739	5.610	5.493	5.389	5.295	5.209	11.235	4.669
0.50	7.364	7.182	7.020	6.875	6.744	6.627	6.520	14.051	5.844
0.60	8.843	8.625	8.431	8.256	8.100	7.958	7.830	16.868	7.020
0.70	11.000	10.746	10.519	10.315	10.133	9.968	9.818	20.362	8.873
0.80	15.300	15.009	14.750	14.518	14.309	14.120	13.950	26.000	12.869
0.90	25.300	24.973	24.681	24.420	24.185	23.973	23.781	37.337	22.565
1.00	35.000	34.637	34.312	34.022	33.761	33.525	33.312	48.375	31.961

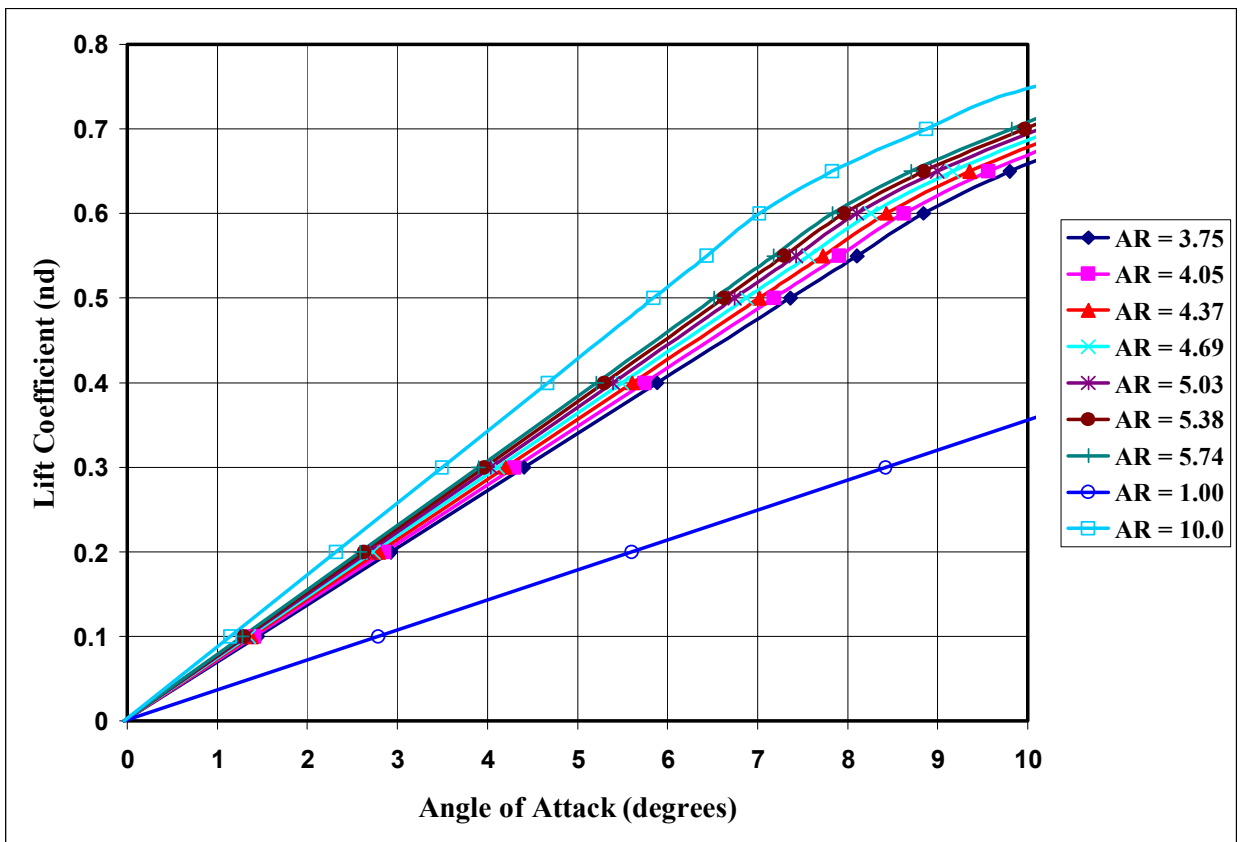


Figure 10. Lift coefficient versus angle of attack for Mach = 0.

Addition of Winglets

For the winglet case, it is assumed that the lift of the wing and winglet combination is the same as that provided by the baseline wing alone, therefore, the baseline lift coefficient and alpha data were used for the baseline aspect ratio. No modifications to the aerodynamic model were needed.

$$C_{L_{WINGLET}} = C_{L_{BASELINE}} \quad (30)$$

Modification of the Drag Polars

Aspect Ratio Changes

From the files contained in DPS of the aircraft lift coefficient and drag coefficient data, Excel files were created. These contain the aerodynamic model over the Mach range of 0.0 to 1.6. For each aspect ratio wing configuration AR-1 through AR-8, the values were converted to the new values using the Lanchester-Prandtl equations (equations 1 and 2). This procedure was used for both the clean (landing gear retracted and wing flaps 0%) and the modified SETOS configuration (landing gear retracted and wing flaps 60%). An example for Mach equal to zero is illustrated in Table 9.

For the case of Mach equal to zero, each of these lift coefficient versus drag coefficient tables was plotted (Figure 11). It can be confirmed that the progression of the modified curves with respect to changes in aspect ratio agrees with theory. As is evident in these new curves, as the aspect ratio increases, the total drag decreases for a given lift coefficient.

Table 9. Lift coefficient and drag coefficient values for Mach = 0.

	Baseline	AR-1	AR-2	AR-3	AR-4	AR-5	AR-6	AR-7	AR-8
C_L	C_D	C_D	C_D	C_D	C_D	C_D	C_D	C_D	C_D
0.00	0.0196	0.0196	0.0196	0.0196	0.0196	0.0196	0.0196	0.0196	0.0196
0.10	0.0199	0.0199	0.0198	0.0198	0.0197	0.0197	0.0196	0.0223	0.0194
0.20	0.0229	0.0227	0.0224	0.0222	0.0220	0.0219	0.0217	0.0322	0.0208
0.30	0.0285	0.0279	0.0274	0.0269	0.0265	0.0262	0.0258	0.0495	0.0237
0.40	0.0406	0.0396	0.0387	0.0379	0.0371	0.0365	0.0359	0.0780	0.0321
0.50	0.0592	0.0577	0.0562	0.0550	0.0538	0.0528	0.0519	0.1176	0.0460
0.60	0.0803	0.0780	0.0760	0.0742	0.0725	0.0710	0.0697	0.1643	0.0612
0.70	0.1074	0.1043	0.1016	0.0991	0.0968	0.0948	0.0930	0.2218	0.0814
0.80	0.1395	0.1355	0.1319	0.1286	0.1257	0.1231	0.1207	0.2889	0.1056
0.90	0.1766	0.1715	0.1669	0.1628	0.1591	0.1557	0.1527	0.3657	0.1336
1.00	0.2186	0.2123	0.2066	0.2015	0.1970	0.1929	0.1891	0.4520	0.1656

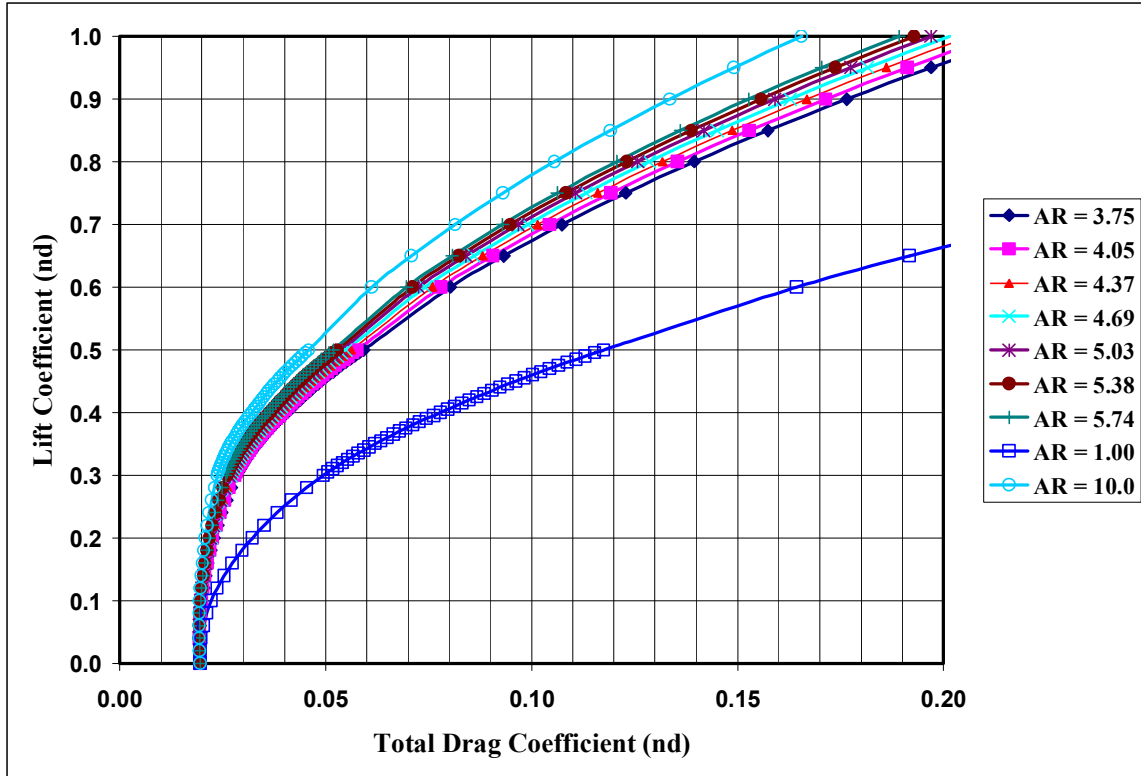


Figure 11. Drag Polars for Mach = 0.

Wing Reference Area Changes

For all modified wing reference areas, the baseline lift coefficient and angle of attack data were used. No modifications to the aerodynamic model were needed. The DPS code was changed to allow for changes in the wing reference area. As previously stated, the lift coefficients used in the induced drag calculations were multiplied by the ratio of baseline wing reference area to the modified values.

Addition of Winglets

From the files contained in DPS of the aircraft lift coefficient and drag coefficient data, Excel spreadsheet data files were created. These files contained the aerodynamic model over the Mach range of 0 to 1.6. For the winglet case, an effective aspect ratio of 1.32 times the baseline aspect ratio ($AR_{BASELINE}$) was calculated. Using this effective aspect ratio ($AR_{EFFECTIVE}$), the values for drag coefficient were converted to the new values using the Lanchester-Prandtl equations (equations 1 and 2).

For subsonic Mach numbers,

$$C_{D_{WINGLET}} = C_{D_{BASELINE}} + \frac{C_{L_{BASELINE}}^2}{\pi} \left(\frac{1}{AR_{EFFECTIVE}} - \frac{1}{AR_{BASELINE}} \right) \quad (31)$$

From Reference 13, for supersonic Mach numbers and lift coefficient greater than 0.2,

$$C_{D_{WINGLET}} = C_{D_{BASELINE}} \quad (32)$$

and for lift coefficients less than 0.2,

$$C_{D_{WINGLET}} = (0.9)C_{D_{BASELINE}} \quad (33)$$

Computer Data Procedures and Run Tables

Aspect Ratio Changes

A flow chart illustrating the DPS procedures for running the simulation for variation in aspect ratios is shown in Figure 12.

Using the flowchart below, data were collected for the aspect ratios wing configurations AR-1 through AR-8 as defined in Table 10.

Wing Reference Area Changes

The DPS run flow chart illustrating the procedures for running the simulation for variation in wing areas is shown in Figure 13.

Using the flowchart below, data were collected for the wing area configurations S-1 through S-6 as defined in Table 11 below.

Addition of Winglets

The DPS flow chart illustrating the procedures for running the winglet simulation is shown in Figure 14.

Using the flowchart below, data were collected for the winglet configuration W-1 as defined by Table 12 below.

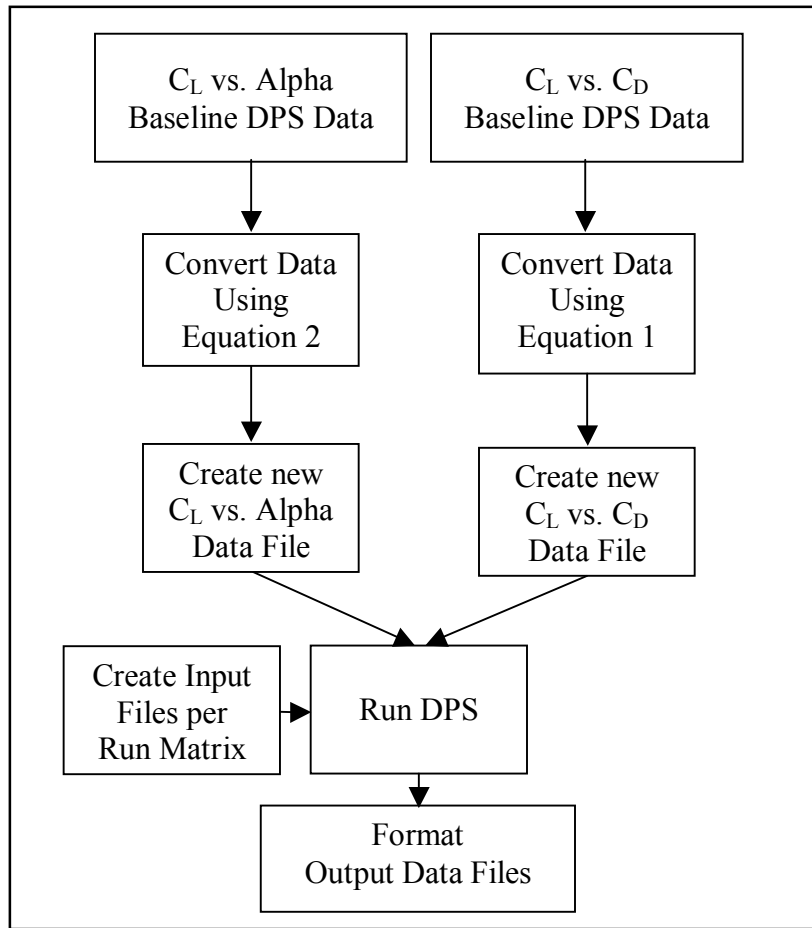


Figure 12. Aspect Ratio Analysis Flowchart

Table 10. Aspect Ratio Run Matrix

Phase	Configuration (Gear/Flaps)	Cases	DPS Maneuver	Start	End	Output
SETOS	Up ¹ / 60%	B ² , AR-1 to AR-8	Level Accel	Mach = 0.2	Mach = 0.5	A/S ³ for P _s ⁴ = 100
SETOS	Up / 60%	B, AR-1 to AR-8	Climb	3500 feet	4500 feet	A/S for P _s = 100
MAX Range	Up / 0%	B, AR-1 to AR-8	Cruise	Mach = 0.7	Mach = 0.9	Specific Range
MAX Speed	Up / 0%	B, AR-1 to AR-8	Max Speed	Mach = 0.9	P _s = 0	Maximum Mach

Notes: 1) “Up” denotes gear retracted and gear doors closed.

2) “B” is Baseline aerodynamic models

3) A/S is calibrated airspeed in knots

4) P_s is specific excess power (feet per minute)

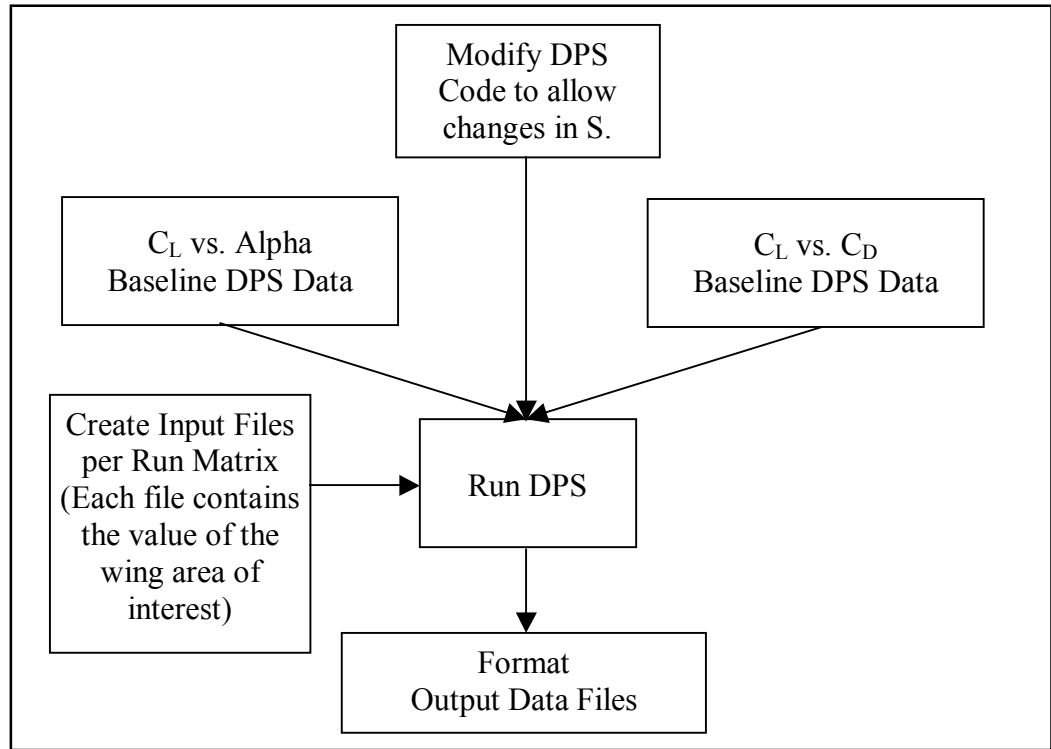


Figure 13. Reference Area Analysis Flowchart

Table 11. Wing Area Run Matrix

Phase	Configuration (Gear/Flaps)	Cases	DPS Maneuver	Start	End	Output
SETOS	Up ¹ / 60%	B ² , S-1 to S-6	Level Accel	Mach = 0.2	Mach = 0.5	A/S ³ for P _s ⁴ = 100
SETOS	Up / 60%	B, S-1 to S-6	Climb	3500 feet	4500 feet	A/S for P _s = 100
MAX Range	Up / 0%	B, S-1 to S-6	Cruise	Mach = 0.7	Mach = 0.9	Specific Range
MAX Speed	Up / 0%	B, S-1 to S-6	Max Speed	Mach = 0.9	P _s = 0	Maximum Mach

- Notes: 1) “Up” denotes gear retracted and gear doors closed.
 2) “B” is Baseline aerodynamic models
 3) A/S is calibrated airspeed in knots
 4) P_s is specific excess power (feet per minute)

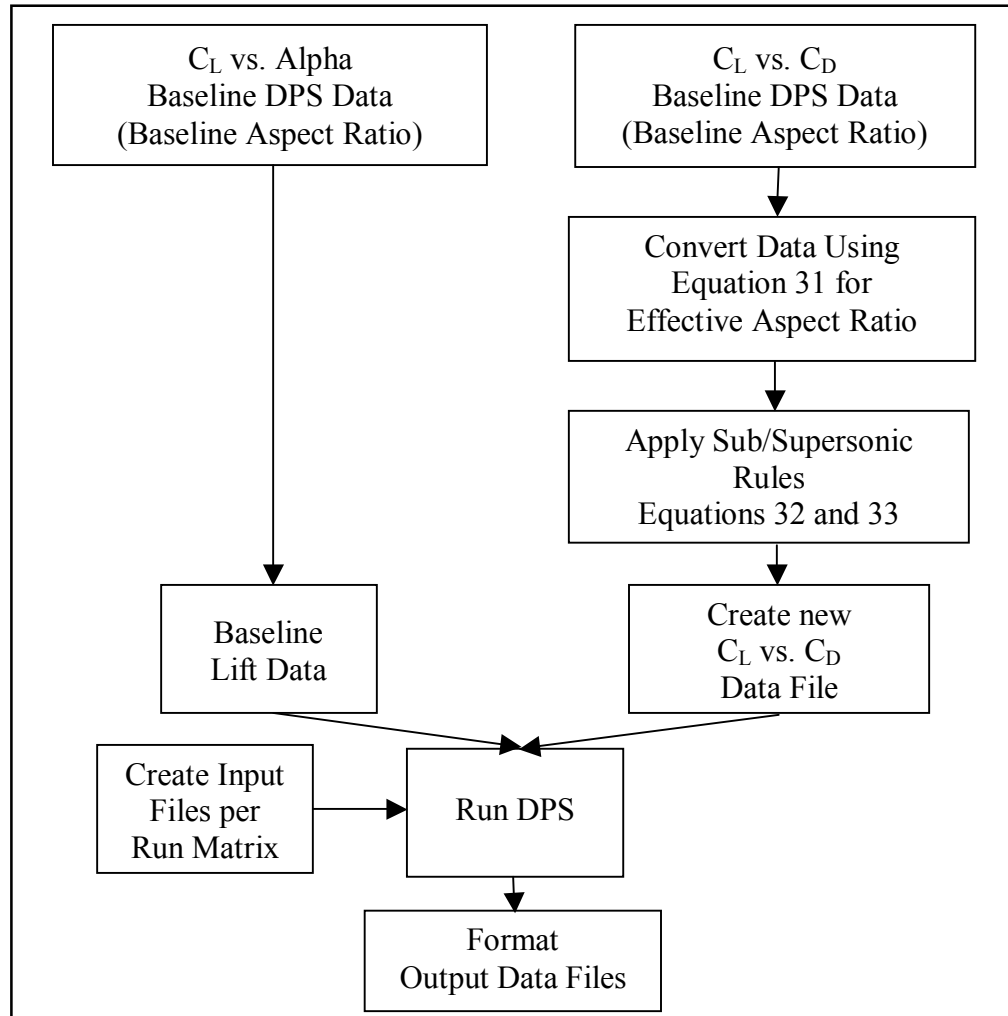


Figure 14. Winglet Analysis Flowchart

Table 12. Winglet Run Matrix

Phase	Configuration (Gear/Flaps)	Cases	DPS Maneuver	Start	End	Output
SETOS	Up ¹ / 60%	B ² , W-1	Level Accel	Mach = 0.2	Mach = 0.5	A/S ³ for P _s ⁴ = 100
SETOS	Up / 60%	B, W-1	Climb	3500 feet	4500 feet	A/S for P _s = 100
MAX Range	Up / 0%	B, W-1	Cruise	Mach = 0.7	Mach = 0.9	Specific Range
MAX Speed	Up / 0%	B, W-1	Max Speed	Mach = 0.9	P _s = 0	Maximum Mach

- Notes: 1) "Up" denotes gear retracted and gear doors closed.
 2) "B" is Baseline aerodynamic models
 3) A/S is calibrated airspeed in knots
 4) P_s is specific excess power (feet per minute)

SETOS

In order to determine the Single Engine Takeoff Speed (SETOS), two separate profiles were run. For each wing configuration, a level acceleration was simulated at 4,000 feet pressure altitude, followed by a separate climb profile from 3,500 feet to 4,500 feet. In each case, the aircraft weight was 13,000 pounds, simulating a fully-fueled aircraft. One engine was set to maximum afterburning thrust, and the other engine was shut-down and windmilling (RPM not zero). Ambient atmospheric air temperature was set at 30 degrees C above standard day temperature (37.1 degrees C or 98.8 degrees F). Fuel burn was set to zero, so that weight remained constant during each run. A sample DPS input data file can be found in Appendix C.

After completing the level acceleration, the data output included specific excess power and velocity. From this data, the approximate velocity for a specific excess power of +100 feet per minute at a normal load factor of 1g could be determined. Using this airspeed value as a starting point, the single engine climb profile was conducted. Since this profile more closely matched the conditions during a single engine takeoff (a normal load factor of less than 1g), it was a better indication of true specific excess power. The airspeed was varied until the value for specific excess power at 4,000 feet was equal to 100 feet per minute. A visual depiction of this iteration can be seen in Figure 15. The red double circle depicts the target specific excess power versus altitude point. In this example, SETOS is approximately 161 KIAS. Using this method, SETOS was found for each configuration.

The variations in each curve that are evident between 3500 and 3700 feet are caused by the algorithms used in the DPS program. These overshoots, however, settle out before the midpoint value of 4000 feet. As a result, valid data points for each airspeed and configuration are obtained by using this 1000 foot interval for each SETOS climb – centered on the altitude of interest.

Maximum Range

In order to determine the maximum range, one profile was run. For each configuration, a level cruise segment was simulated at a constant 30,000 feet pressure altitude. Constant altitude cruise is more operationally representative of this training aircraft's typical cruise contour as opposed to a climb-cruise profile. In each case, the aircraft weight was 10,000 pounds, simulating an aircraft nearing the end of a navigation cruise. Ambient temperature was standard day value from the 1976 U.S. Standard Atmosphere. Fuel burn was set to zero, so weight remained constant during each run. An example DPS input data file can be found in Appendix C.

After completing the cruise, the data output included Mach number and specific range (SR). These data were plotted, and the maximum value of specific range could be determined.

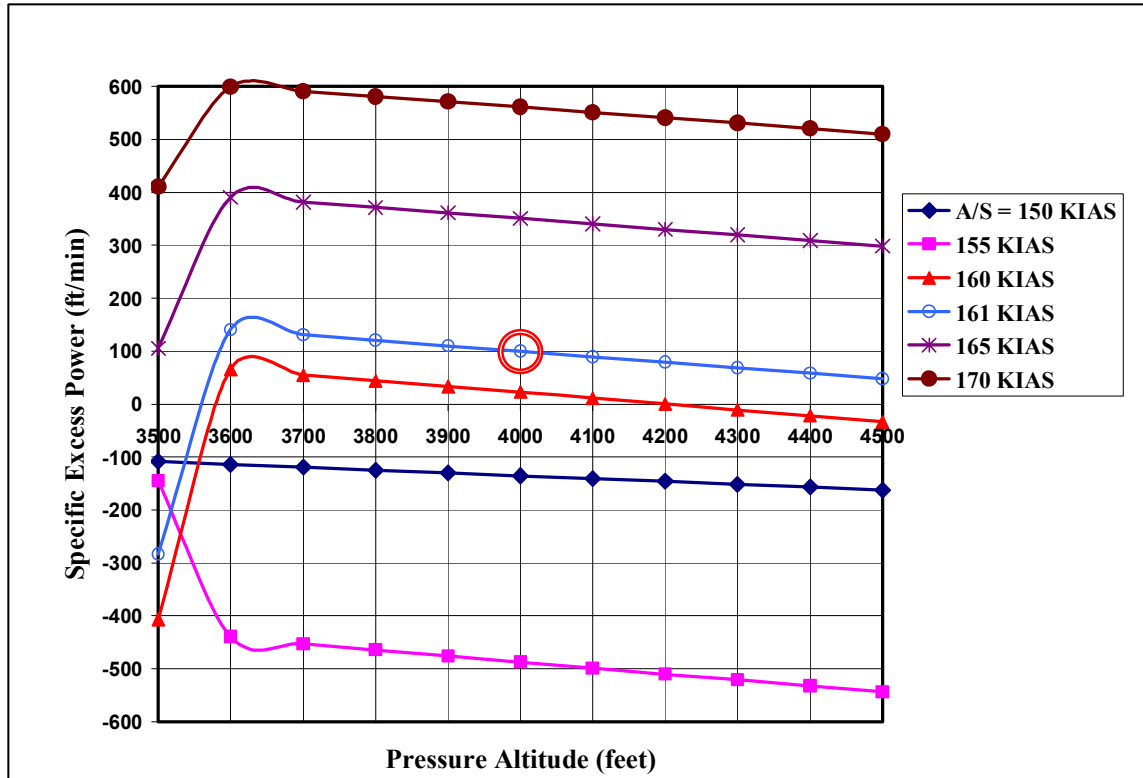


Figure 15. SETOS iteration example.

Maximum Speed

In order to determine the maximum speed, one profile was run for each configuration. A constant altitude cruise segment was simulated at various altitudes from zero feet pressure altitude to 45,000 feet pressure altitude. For each altitude and starting from 0.7 Mach, the maximum Mach number was computed for zero excess thrust with both engines set at maximum afterburning thrust. In each case, the aircraft weight was 10,000 pounds. Ambient temperature was standard day value from the 1976 U.S. Standard Atmosphere. Fuel burn was set to zero, so weight remained constant during each run. An example DPS input data file can be found in Appendix C.

After completing each point, the data output included altitude and maximum Mach number. This data was plotted as a maximum speed versus altitude profile.

Minimum Speed

All calculations for T-38C stall speed were performed analytically and did not require the use of DPS.

Error Analysis

The original flight test data used to construct the models used by DPS were accurate to approximately ± 100 feet per minute (less than 1.66 feet per second). Despite the fact that this error is the same as the definition of SETOS, valid analysis can be conducted. This error is not significant for the maximum range and maximum speed studies as well.

RESULTS AND DISCUSSION

Takeoff

All SETOS data points were successfully obtained. In all cases, SETOS performance was improved by using winglets, or increasing aspect ratio or wing area above the baseline value.

Aspect Ratio Results

The aspect ratio results are summarized in Table 13.

For an aspect ratio of 1.00 (AR-7), SETOS is not possible. Here, the induced drag prevents a successful single-engine takeoff regardless of the airspeed. From the simulation, the maximum specific excess power reached was approximately -300 feet per minute – well below the required +100 feet per minute definition of SETOS.

Graphically (Figure 16), it can be seen that the SETOS versus aspect ratio curve is asymptotic as aspect ratio increases. So, as the aspect ratio is increased, the incremental gains in SETOS become smaller and eventually reach a steady state value. The largest SETOS gain for the smallest amount of aspect ratio increase occurs from the baseline to the AR-1 wing configuration.

Wing Area Results

The results for the wing area are listed in Table 14.

Graphically (Figure 17), it can be seen that the curve is asymptotic as wing area increases. So, as the wing area is increased, the gains in SETOS become smaller and eventually reach a steady state value. The largest incremental gain occurs from baseline to S-1.

Winglet Results

The results for the winglet are listed in Table 15.

By plotting this point (see Figure 18) on the previous graph for aspect ratio (Figure 18), it should be noted that the winglet design, as modeled in this study, yields an incremental improvement in SETOS over the baseline aspect ratio value. This is determined by noting that the location of the single data point lies well below the handfired trendline of the aspect-only data points. When compared to the baseline aspect ratio, the winglet design provides an incremental decrease in SETOS of just over 3 knots.

Table 13. SETOS values for varying aspect ratios.

AR	Actual AR	SETOS (KIAS)
Baseline	3.75	161.0
AR-1	4.05	159.9
AR-2	4.37	159.2
AR-3	4.69	158.6
AR-4	5.03	158.0
AR-5	5.38	157.4
AR-6	5.74	156.9
AR-7	1.00	Not Possible
AR-8	10.00	154.3

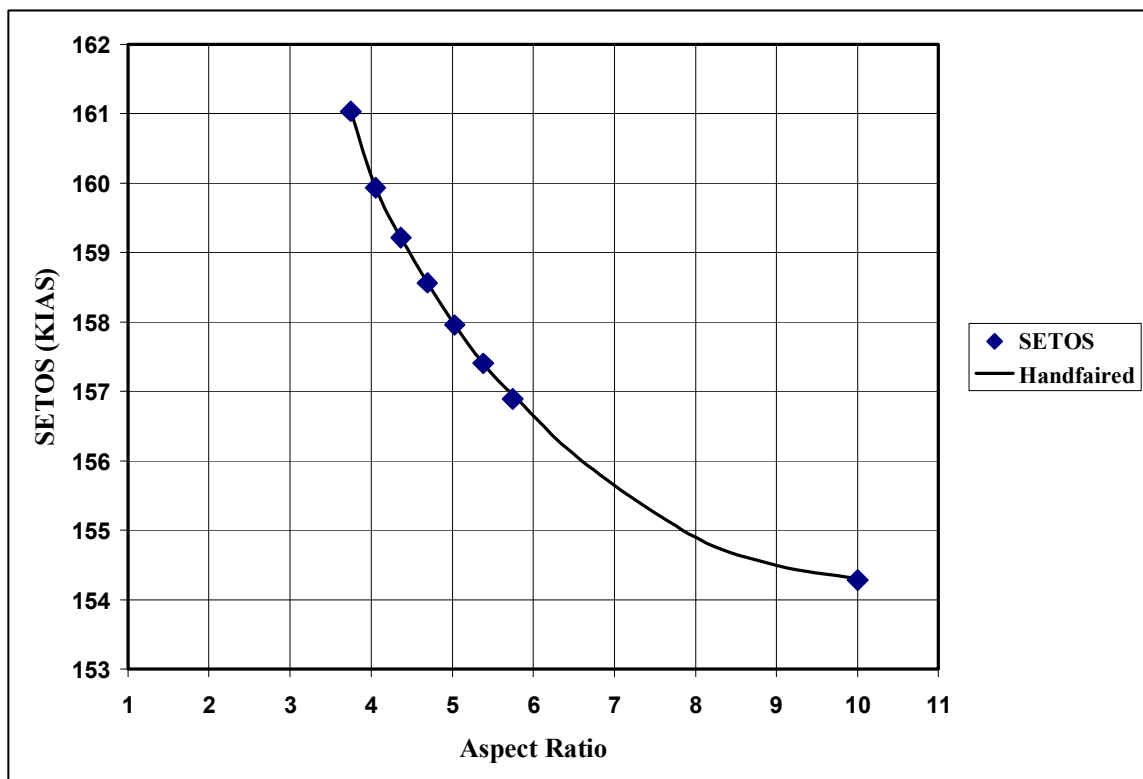


Figure 16. SETOS trend versus aspect ratio.

Table 14. SETOS values for varying wing areas.

Wing Configuration	S (sq feet)	SETOS (KIAS)
Baseline	170.0	161.0
S-1	183.7	150.7
S-2	198.0	141.4
S-3	212.8	135.4
S-4	228.1	131.8
S-5	244.0	129.3
S-6	260.4	127.6

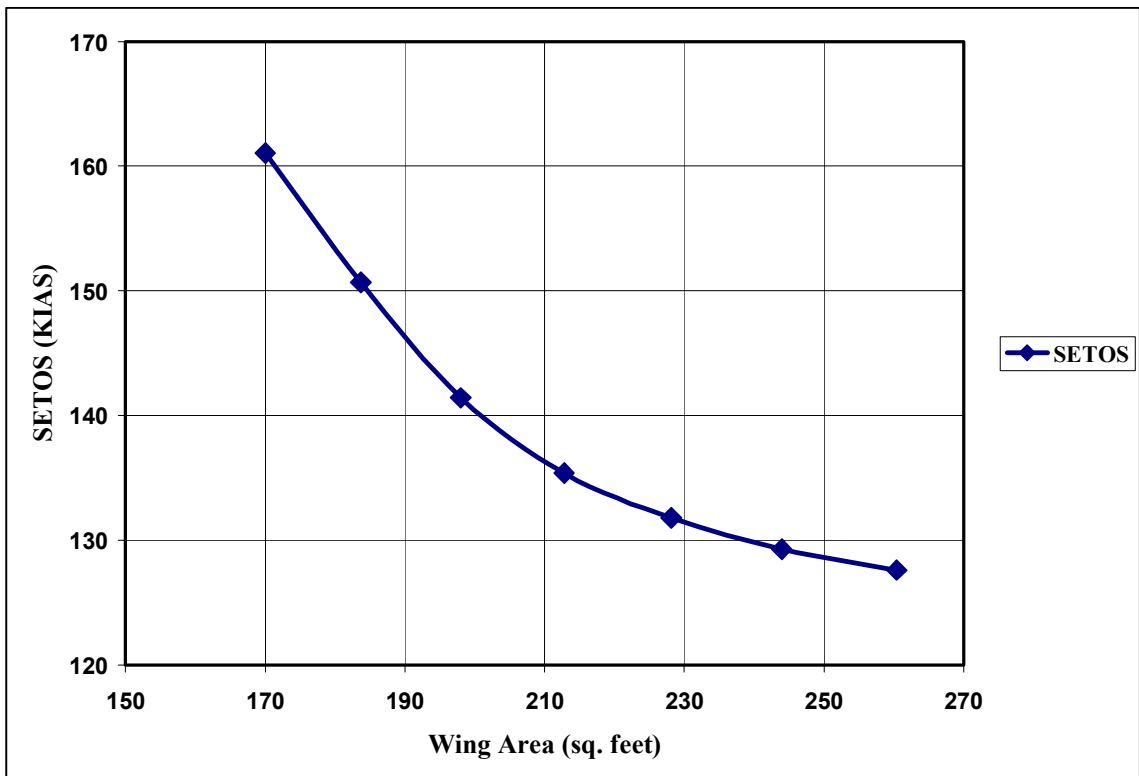


Figure 17. SETOS trend versus wing area.

Table 15. SETOS values for wing-winglet combination.

Wing Configuration	Actual AR	Effective AR	SETOS (KIAS)
Baseline	3.750	N/A	161.0
W-1	3.750	4.960	157.8

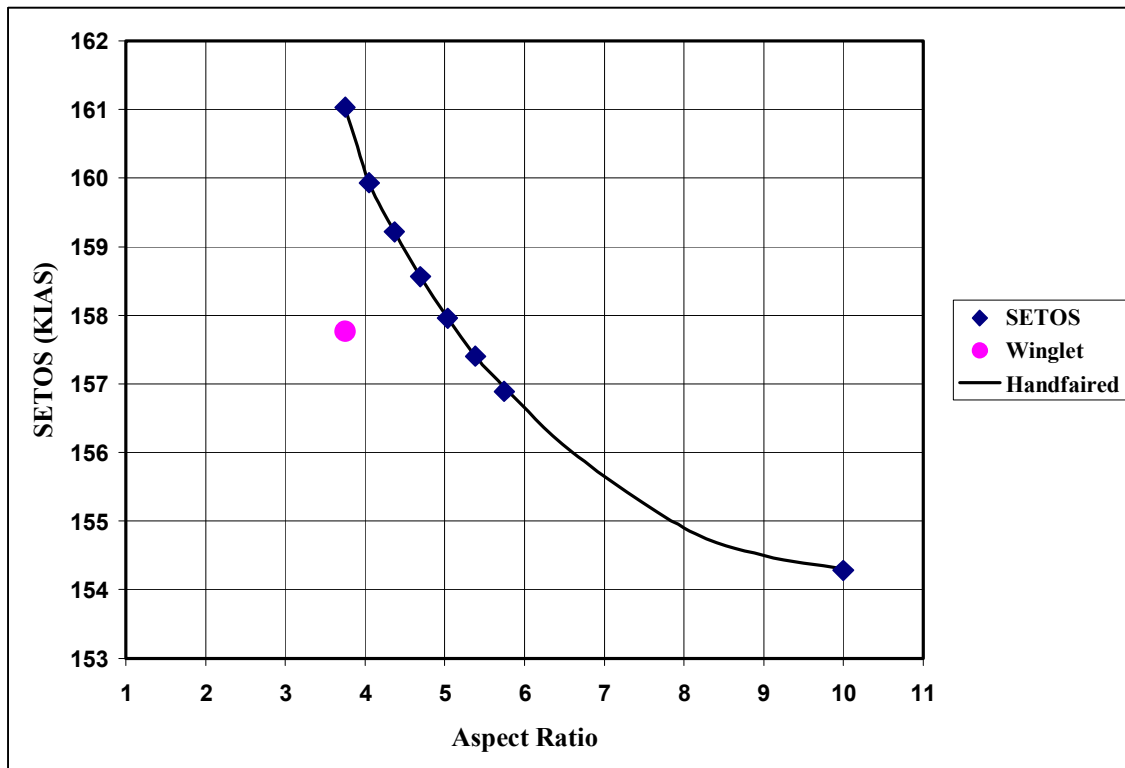


Figure 18. SETOS trend versus aspect ratio with winglet point added.

Cruise

Maximum Range

Maximum specific range was successfully determined for all points.

Aspect Ratio Results

As expected, maximum specific range increased with increases in aspect ratio and decreased for the aspect ratio of 1.00. The values for Mach versus specific range were plotted for each case (Figure 19). As depicted below, as aspect ratio increased, the maximum value for specific range increased and occurred at a lower Mach number. This is due to the increase in overall lift-to-drag ratio caused by the decrease in induced drag.

Specific range is given in nautical air miles per pound of fuel (nam/lb). The maximum points are summarized in Table 16. Plotting maximum specific range versus aspect ratio yields Figure 20. Again, this graph (Figure 20) is asymptotic with increase in aspect ratio and will eventually reach a maximum value. From the limited points of this study, it can be seen that significant increases (greater than approximately 100 nautical air miles) in the operational range of the T-38 are not possible.

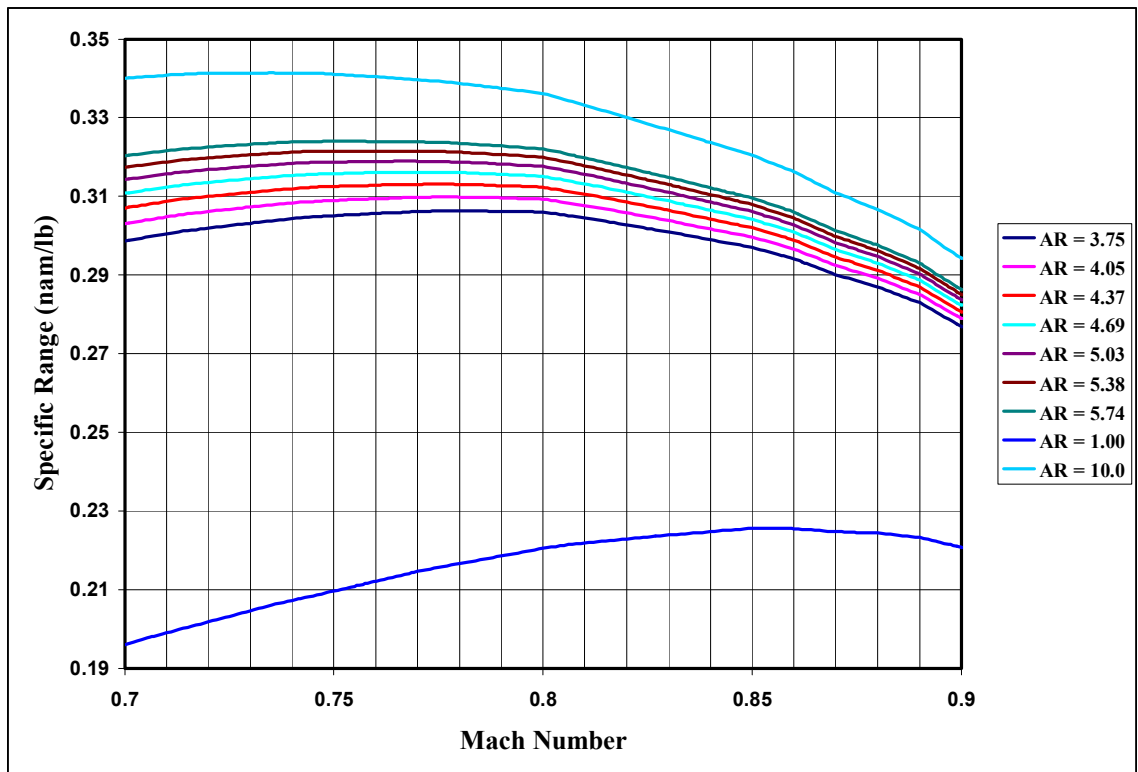


Figure 19. Specific range plots for variation in aspect ratio.

Table 16. Variation of maximum specific range with aspect ratio.

Wing Configuration	Actual AR	Max SR (nam/lb)	Mach Number
Baseline	3.75	0.3063	0.778
AR-1	4.05	0.3099	0.776
AR-2	4.37	0.3131	0.776
AR-3	4.69	0.3161	0.775
AR-4	5.03	0.3189	0.767
AR-5	5.38	0.3215	0.759
AR-6	5.74	0.3240	0.751
AR-7	1.00	0.2256	0.852
AR-8	10.00	0.3414	0.735

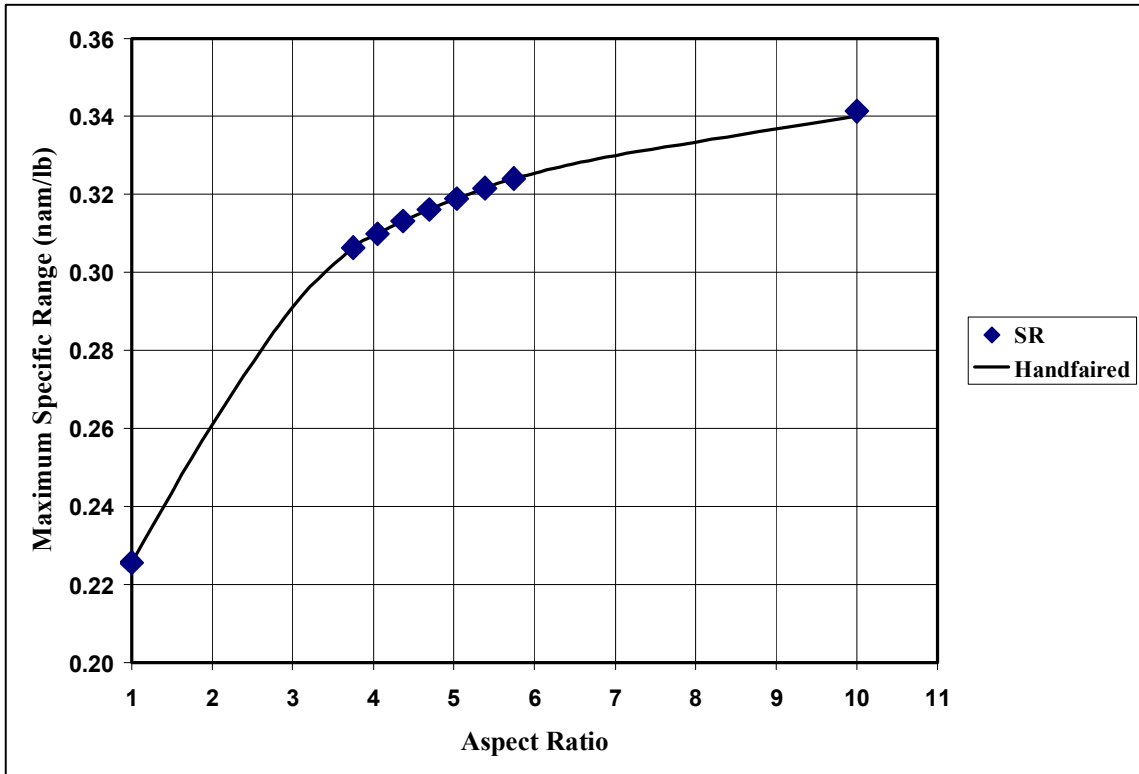


Figure 20. Maximum specific range variation with aspect ratio.

Wing Area Results

As expected, maximum specific range increased with increases in wing area. The values for Mach versus specific range were plotted for each case (Figure 21). As before, increases in wing area reduced drag and increased the lift-to-drag ratio. This caused the peak of each curve to be shifted up (higher values of maximum specific range) and to the left (maximum value occurred at lower Mach numbers).

The maximum specific range points are summarized in Table 17. Plotting maximum specific range versus wing area yields Figure 22. In this case, from the limited points of this study, it can be seen that significant increases (greater than approximately 100 nautical air miles) in the operational range of the T-38 are possible, but only with a large increase in wing area.

Winglet Results

As expected, maximum specific range increased with the addition of the winglet. The values for Mach versus specific range were plotted for this case (Figure 23). As before, the decrease in drag caused the maximum value to increase and the Mach number at which this occurred to decrease.

The maximum specific range points are summarized in Table 18. Plotting maximum specific range versus aspect ratio yields Figure 24. The maximum range value for the winglet provides an incremental gain in maximum specific range. This is determined by noting that the location of the single data point lies above the handfaired trendline of the aspect-only data points. When compared to the baseline aspect ratio, the winglet design provides a positive incremental gain in maximum specific range of approximately 0.0119 nautical air miles per pound of fuel.

Maximum Speed

Maximum speed profiles were determined for all points. It is assumed that the airframe would have been modified with optimum area-ruling. In general, modifications that decreased total drag caused increases in maximum speed. Maximum speed occurred where specific excess power equaled zero, in other words, when thrust equaled drag. By decreasing drag and keeping thrust constant, this point would occur at a higher airspeed with any decreases in drag.

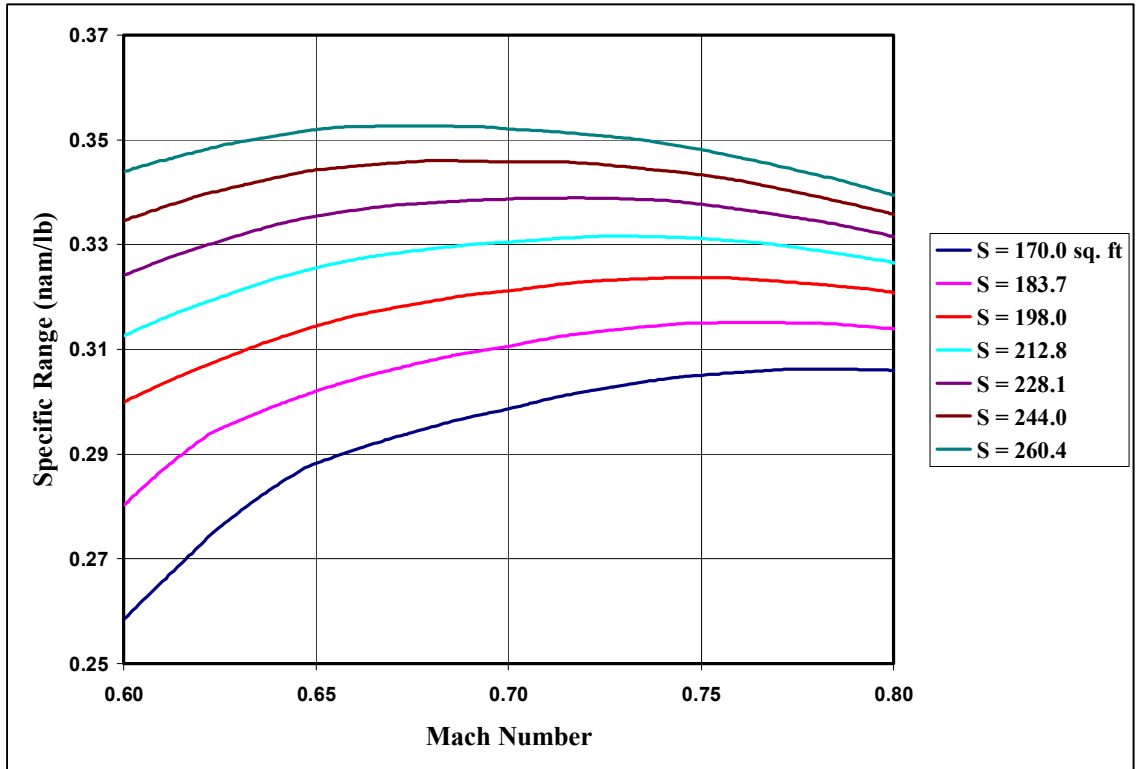


Figure 21. Specific range plots for variation in wing area.

Table 17. Variation of maximum specific range with wing area.

Wing Configuration	S (sq. feet)	Max SR (nam/lb)	Mach Number
Baseline	170.0	0.3063	0.778
S-1	183.7	0.3152	0.763
S-2	198.0	0.3238	0.751
S-3	212.8	0.3317	0.727
S-4	228.1	0.3390	0.716
S-5	244.0	0.3460	0.681
S-6	260.4	0.3527	0.675

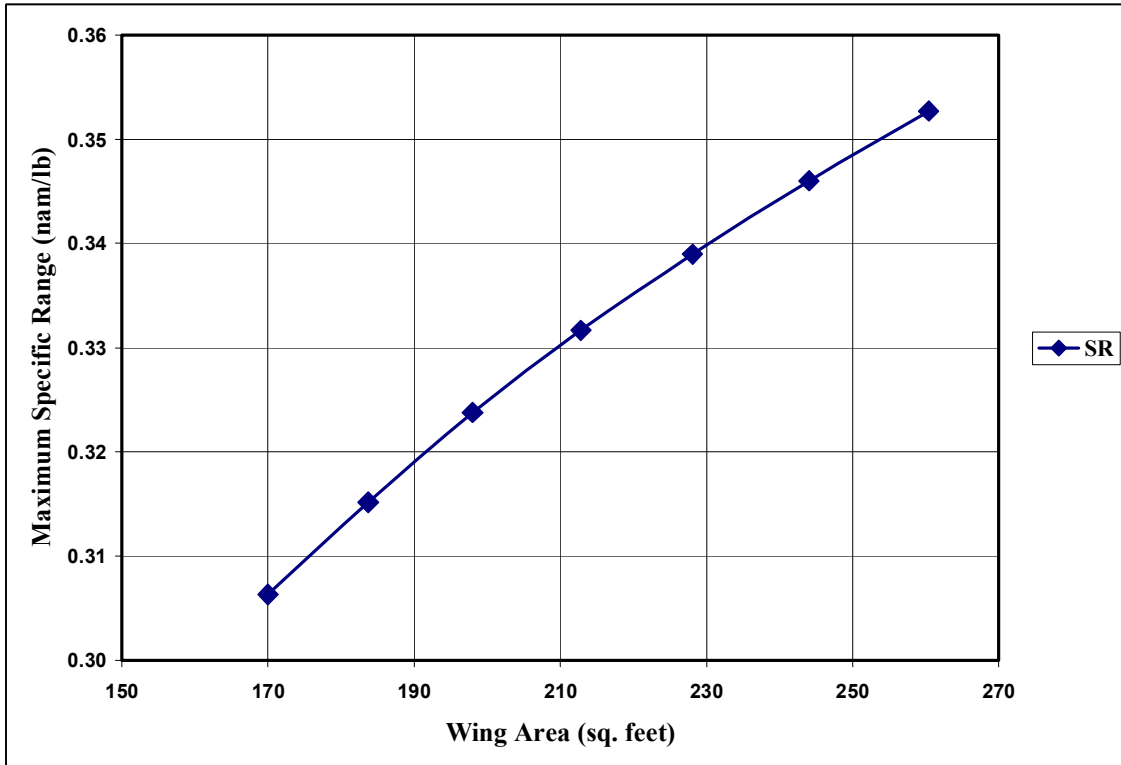


Figure 22. Maximum specific range variation with wing area.

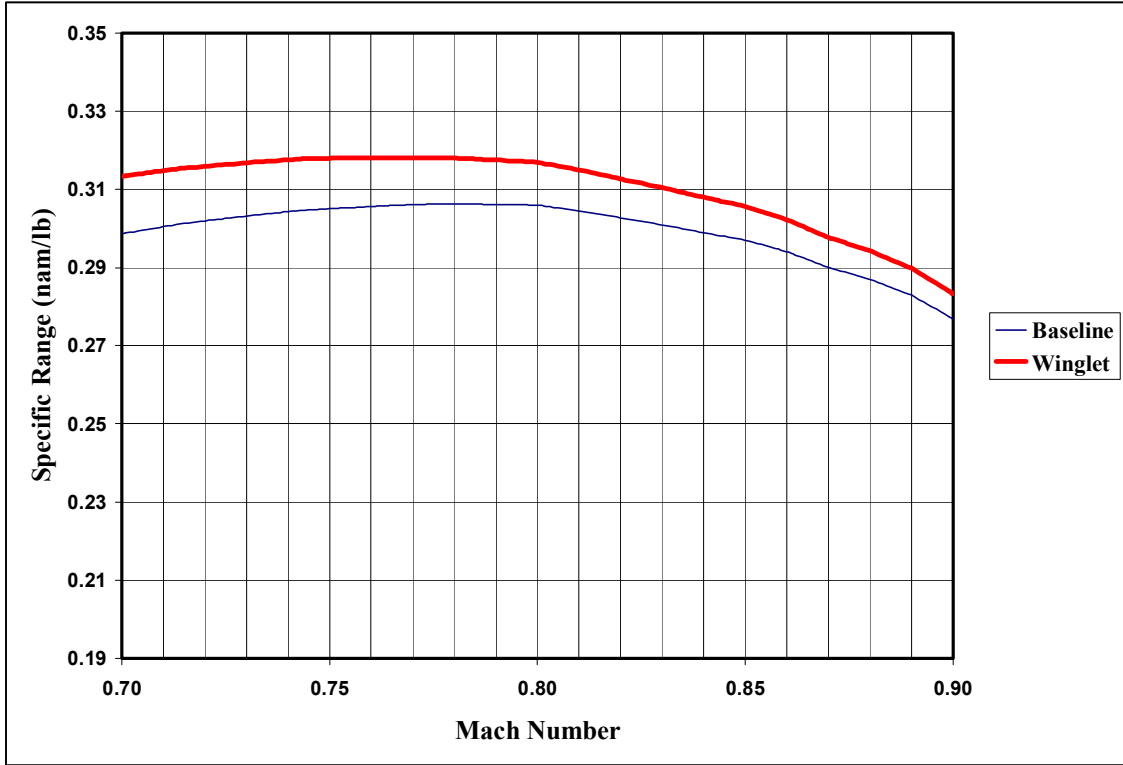


Figure 23. Specific range plots for baseline and winglet.

Table 18. Variation of maximum specific range with winglet added.

AR	Actual AR	Effective AR	Max SR (nam/lb)	Mach Number
Baseline	3.75	N/A	0.3063	0.778
W-1	3.75	4.96	0.3182	0.770

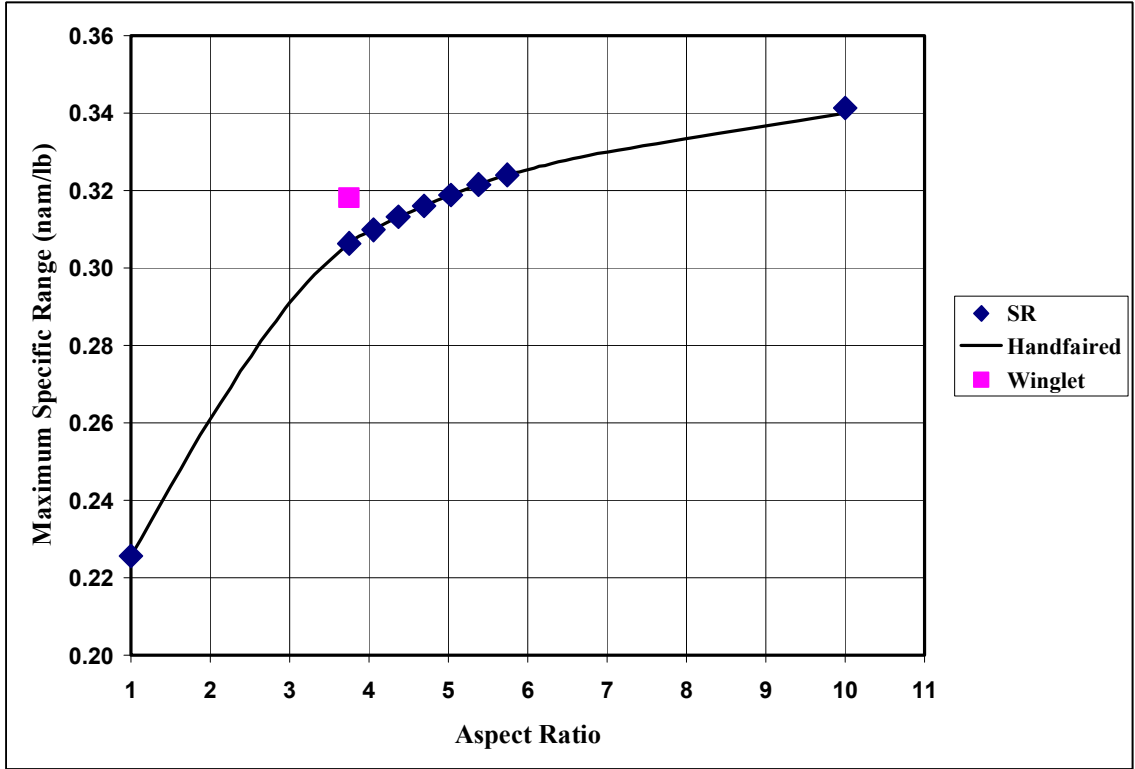


Figure 24. Maximum specific range with winglet.

Aspect Ratio Results

Maximum speed increased with the increase in aspect ratio. For the aspect ratio 1.00 case, the maximum speed actually decreased due to higher drag values. The maximum speed profiles are depicted in Figure 25.

The maximum values are summarized in Table 19. Except for the aspect ratio of 1.00, all maximum values occurred at approximately 36,000 feet.

Wing Area Results

The maximum speed profiles are depicted in Figure 26. From this graph, it appears that maximum speed increased with the increases in wing area. This is due to the fact that the DPS program did not account for the increases in parasite drag caused by the larger wing area. The increase in parasite drag with increasing wing area would result in a decrease in the maximum airspeed of the aircraft.

The maximum values are summarized in Table 20. All maximum values occurred at approximately 36,000 feet.

Winglet Results

Maximum speed was not changed over the baseline aircraft with the addition of the winglets. Based on the model used in this analysis, this was as expected. Except for lift coefficients less than 0.2, the drag coefficient with the winglet was the same as that without. This profile is depicted in Figure 27.

The maximum values are summarized in Table 21. The maximum values both occur at approximately 36,000 feet.

Landing

Stall Speed

Aspect Ratio Results

From the analytical discussion, the stall speed depends only on variations in wing area. Therefore, stall speed and landing distances are not affected by changes in aspect ratio.

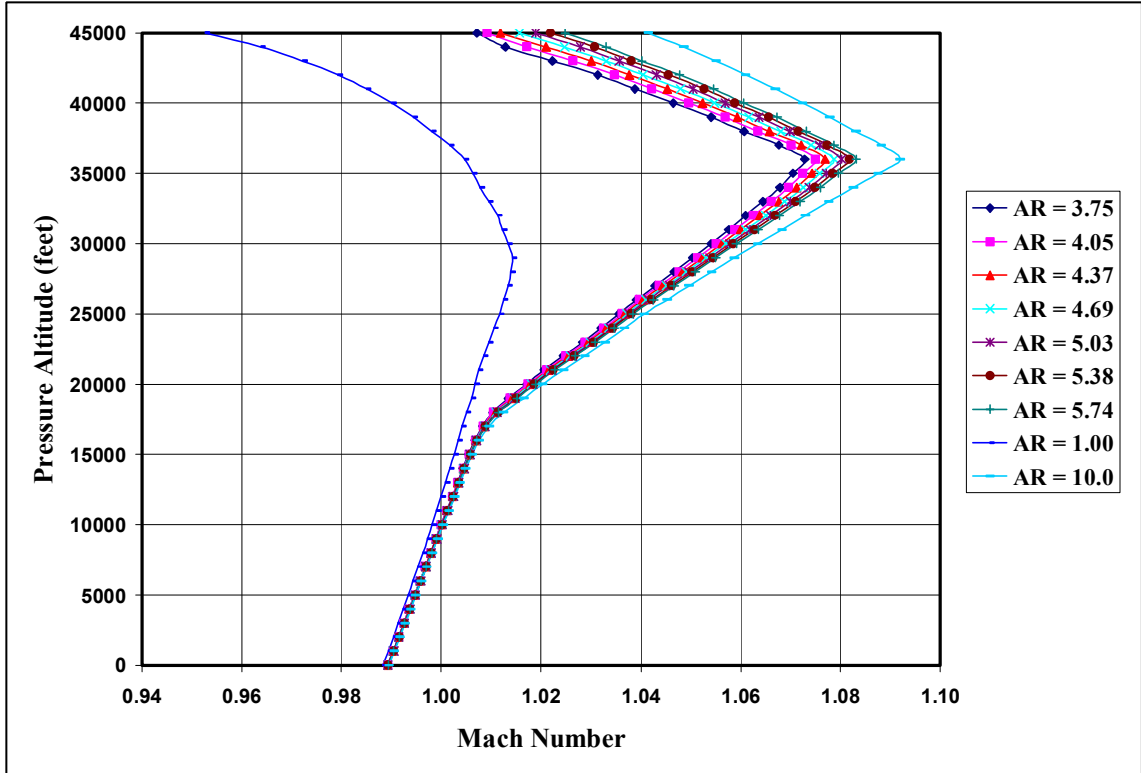


Figure 25. Maximum speed profile for variations in aspect ratio.

Table 19. Maximum Mach numbers for variation in aspect ratio.

Wing Configuration	Max Speed (Mach Number)
Baseline	1.073
AR-1	1.075
AR-2	1.077
AR-3	1.079
AR-4	1.080
AR-5	1.082
AR-6	1.083
AR-7	1.005
AR-8	1.092

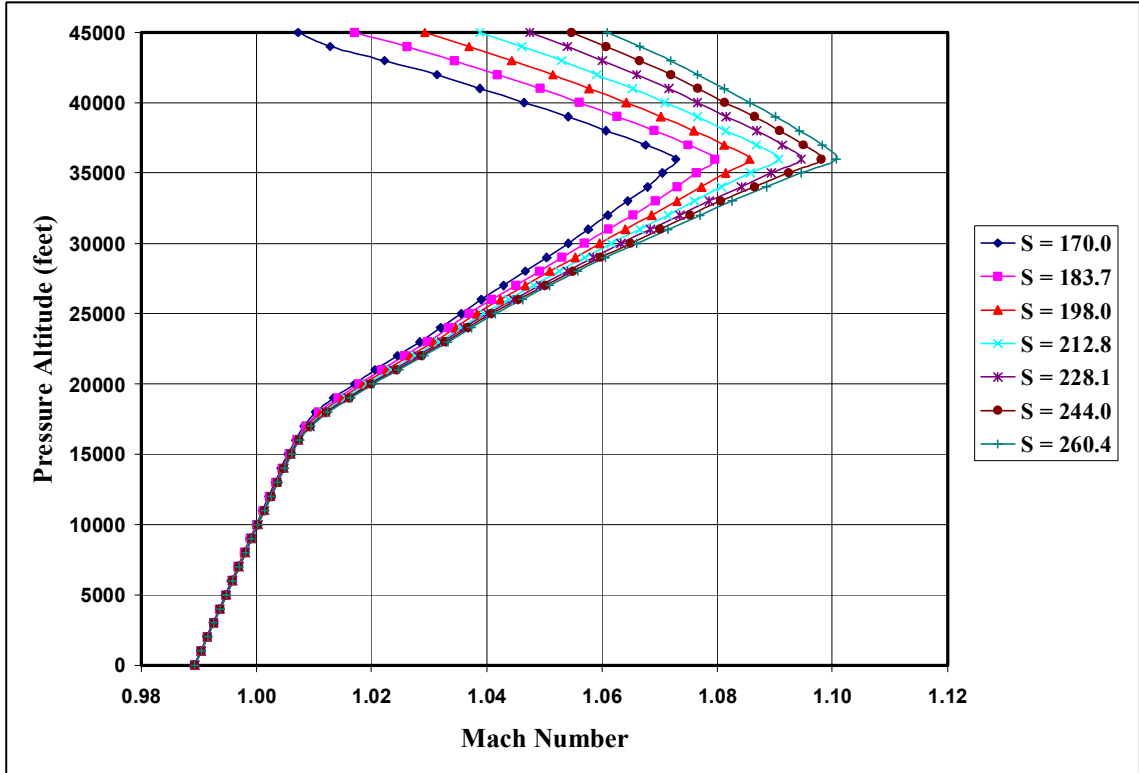


Figure 26. Maximum speed profile for variations in wing area.

Table 20. Maximum Mach numbers for variation in wing area.

Wing Configuration	Maximum Speed (Mach Number)
Baseline	1.073
S-1	1.080
S-2	1.086
S-3	1.091
S-4	1.095
S-5	1.098
S-6	1.101

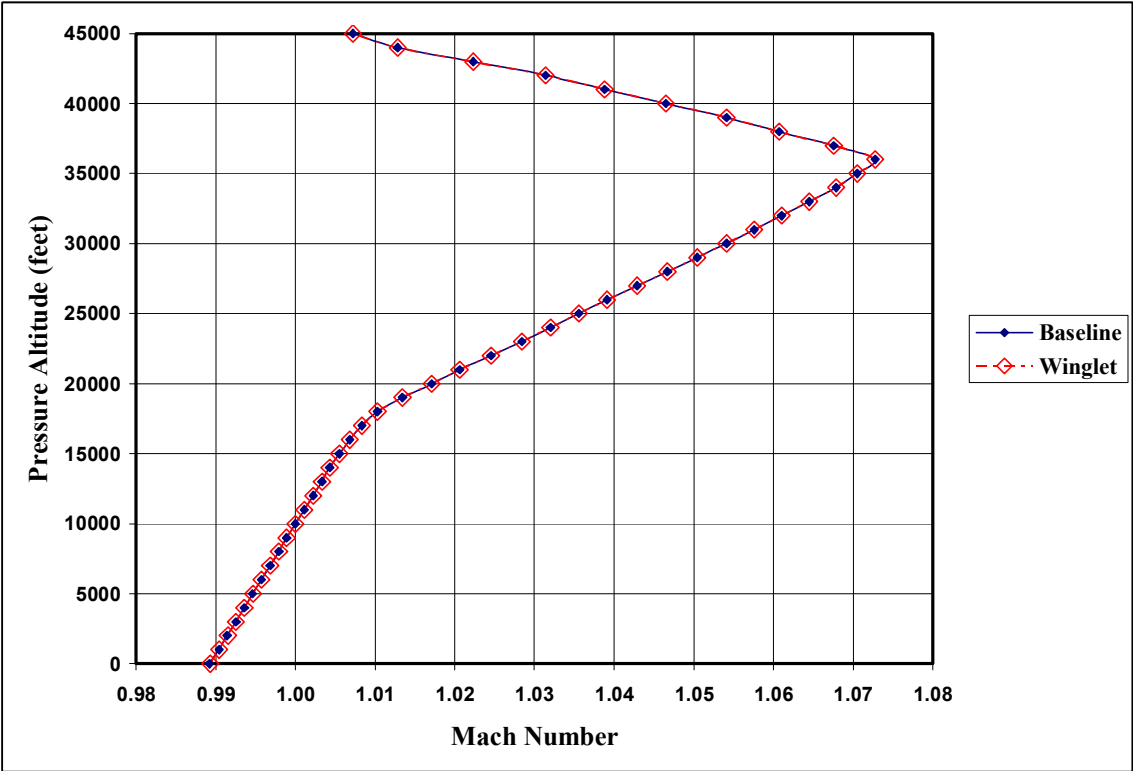


Figure 27. Maximum speed profile with winglet.

Table 21. Maximum Mach number with winglet.

AR	Max Speed (Mach Number)
Baseline	1.073
W-1	1.073

Wing Area Results

For a 12,500 pound T-38C, at 7.5 degrees C, 4,000 feet pressure altitude, and flaps set to 60%, the stall speed is 152 KIAS (Reference 10). Also from Reference 10, this yields a landing speed of 163 KIAS. These conditions result in a stall margin of 1.072 and a landing distance of 6,000 feet. This example simulates a landing immediately after takeoff, perhaps due to an emergency.

If the stall margin is constant, the results can be compiled in Table 22.

For a 9,700 pound T-38C, at 7.5 degrees C, 4,000 feet pressure altitude, and flaps set to 100%, the stall speed is 133 KIAS (Reference 8). Also from Reference 8, this yields a landing speed of 134 KIAS. This equals a stall margin of 1.008. The landing distance in this case is 4,200 feet. This example simulates a normal landing at the end of a sortie.

Again, if the stall margin is again assumed constant, the results can be compiled in Table 23.

Winglet Results

From the analytical discussion, for the purposes of this report, stall speed depends only on variations in wing area. Therefore, stall speed and thus landing distances are not affected by the addition of winglets.

Wing Weights

From the data, it would appear that the best solution would be to replace the T-38 wing with one with a large aspect ratio, a large surface area, and winglets. These improvements, however, all add weight to the aircraft. From Reference 8, the weight gain can be approximated by:

$$w_{WING} = \left[\left(\frac{S'}{S_{REF}} \right)^{0.622} \left(\frac{AR'}{AR_{REF}} \right)^{0.785} \right] w_{WING_{REF}} \quad (34)$$

The current weight of the T-38 wing is 2,795 lbs. The weight of the winglet design is more difficult to model. Therefore, for comparison purposes, it is assumed that it would weigh the same as a wing with the same effective aspect ratio, although in fact, it could be substantially lower.

Table 22. Effect of wing area changes on stall speed, landing speed, and landing distance for 12,500 lbs.

Wing Configuration	S (sq ft)	$\frac{S_{REF}}{S}$	Stall Speed (KIAS)	Landing Speed (KIAS)	Stall Margin	Landing Distance (feet)
Baseline	170.0	1.000	152	163	1.072	6000
S-1	183.7	0.925	146	157	1.072	5552
S-2	198.0	0.859	141	151	1.072	5152
S-3	212.8	0.799	136	146	1.072	4793
S-4	228.1	0.745	131	141	1.072	4471
S-5	244.0	0.697	127	136	1.072	4180
S-6	260.4	0.653	123	132	1.072	3917

Note: T-38C, 12,500 lbs, 7.5 deg C, 4,000' PA, flaps 60%.

Table 23. Effect of wing area changes on stall speed, landing speed, and landing distance for 9,700 lbs.

Wing Configuration	S (sq ft)	$\frac{S_{REF}}{S}$	Stall Speed (KIAS)	Landing Speed (KIAS)	Stall Margin	Landing Distance (feet)
Baseline	170.0	1.000	133	134	1.008	4200
S-1	183.7	0.925	128	129	1.008	3886
S-2	198.0	0.859	123	124	1.008	3606
S-3	212.8	0.799	119	120	1.008	3355
S-4	228.1	0.745	115	116	1.008	3130
S-5	244.0	0.697	111	112	1.008	2926
S-6	260.4	0.653	107	108	1.008	2742

Note: T-38C, 9,700 lbs, 7.5 deg C, 4,000' PA, flaps 100%.

Note that from equation 34, the wings of greater aspect ratio increase weight more quickly than increasing the wing surface area. This is due to the fact that wings of longer span have higher bending moments and therefore require more physical structure to support the wing lift distributions.

The weight increases for the cases in the present study are listed in Tables 24 and 25.

Table 24. Weight of proposed wings for varying aspect ratio.

Wing Configuration	AR (nd)	$\frac{AR}{AR_{REF}}$	Wing Weight (lbs)	Weight Change (lbs)
Baseline	3.75	1.00	2795	0
AR-1	4.05	1.08	2971	176
AR-2	4.37	1.16	3150	355
AR-3	4.69	1.25	3334	539
AR-4	5.03	1.34	3521	726
AR-5	5.38	1.44	3712	917
AR-6	5.74	1.53	3906	1111
AR-7	1.00	0.27	990.0	-1805
AR-8	10.00	2.67	6036	3241
W-1	4.96	1.32	3481	686

Table 25. Weight of proposed wings for varying wing areas.

Wing Configuration	S (sq ft)	$\frac{S}{S_{REF}}$	Wing Weight (lbs)	Weight Change (lbs)
Baseline	170.0	1.00	2795	0
S-1	183.7	1.08	2933	138
S-2	198.0	1.16	3073	278
S-3	212.8	1.25	3214	419
S-4	228.1	1.34	3356	561
S-5	244.0	1.44	3499	704
S-6	260.4	1.53	3644	849

SUMMARY OF RESULTS

The incorporation of a different wing design will require modifications to the existing airframe. Although continued increases in performance were observed as both aspect ratio and wing area were increased, the feasibility of attaching these wings to the T-38 decreased. In order to minimize the required airframe structural changes, the various areas of performance of only the AR-1, S-1, and W-1 configurations were compared.

SETOS

Except for the aspect ratio equal to 1.00 case, all configurations in the present study decreased the induced drag of the wing. Since induced drag is the largest contributor to the total drag at low airspeeds, the effects of the wing changes were most pronounced in the SETOS results (Table 26).

Improvements in SETOS can also be seen as increases in the maximum temperature that would yield the same airspeed value as the baseline. To obtain these values, DPS profiles were run with the baseline value of SETOS as the climb speed and the temperature were varied until the specific excess power equaled 100 feet per minute at 4,000 feet pressure altitude. A summary of the temperature gains in SETOS for wing configurations AR-1, S-1, and W-1 (Table 27) is listed below.

From Table 27, it can be seen that a baseline aircraft will have a SETOS of 161 KIAS at 98.8 degrees F, but a T-38 with the S-1 wing will have lower SETOS until the ambient temperature reaches 153.6 degrees F. This clearly illustrates that a small gain in wing area produces a significant gain in the operational envelope of the aircraft.

Maximum Range

The range is given by the following equation.

$$Range = (SR)w_{fuel} \quad (35)$$

For a typical T-38C mission, a total of approximately 4,000 pounds of fuel are available. After taking into account fuel used for taxi, takeoff, climb, approach, landing, and reserves, approximately 2000 pounds remain for the navigation portion of a mission.

Therefore, using equation 35 with the weight of fuel equal to 2000 pounds, a summary of the distances achieved for wing configurations AR-1, S-1, and W-1 are in Table 28.

For these three cases, the greatest range gained is for the winglet case. Here, the addition of the winglets improves the maximum range by approximately 23 nautical air miles or a gain of approximately 3.9%. This is not operationally significant for a trainer aircraft.

Table 26. Summary of SETOS results.

Configuration	SETOS (KIAS)
Baseline	161.0
AR-1	159.9
W-1	157.8
S-1	150.7

Table 27. Equivalent temperatures for baseline SETOS values.

Configuration	SETOS (KIAS)	Equivalent Temperature Above Standard-Day (degrees C)	Equivalent Ambient Temperature for 4,000 feet (degrees C)	Equivalent Ambient Temperature for 4,000 feet (degrees F)
Baseline	161.0	30.0	37.1	98.8
AR-1	161.0	34.5	41.6	106.9
W-1	161.0	45.8	52.9	127.2
S-1	161.0	60.4	67.6	153.6

Table 28. Maximum range summary for a 2000 pound fuel burn.

Configuration	SR (nam/lb)	Range (nam)
Baseline	0.3063	613
AR-1	0.3099	620
W-1	0.3182	636
S-1	0.3152	630

Maximum Speed

All of the configurations allowed the aircraft to achieve supersonic maximum speeds. All configurations, except for the aspect ratio 1.00 case, had their peak speeds at approximately 36,000 feet (Table 29). From the Standard Atmosphere, the temperature becomes constant above this altitude. As altitude continues to increase, density decreases and therefore, total thrust decreases. As a result, maximum speed decreases as well.

None of the cases however, produced operationally significant changes in the maximum overall maximum speed.

Landing Distances

As detailed in Table 30, only the increases in wing area reduced the landing distances of the aircraft.

For both the heavy weight and light-weight cases, a small increase in wing area reduced the landing distances by approximately 7.5%.

Table 29. Maximum speed summary.

Configuration	Maximum Speed (Mach Number)
Baseline	1.073
AR-1	1.075
W-1	1.073
S-1	1.080

Table 30. Landing distance summary.

Configuration	Landing distance Heavy weight, 60% flap (ft)	Landing distance Light weight, 100% flap (ft)
Baseline	6000	4200
AR-1	6000	4200
W-1	6000	4200
S-1	5552	3886

CONCLUSIONS

Using the Digital Performance Simulation aircraft-performance computer code, a T-38C performance evaluation sensitivity study was performed by parametrically varying the wing design. The computer model was a three degree of freedom, point-mass, batch simulation. The design changes investigated included varying aspect ratio with constant wing area, varying wing area with constant aspect ratio, and the addition of a winglet. These preliminary design estimates compared the differences in takeoff, cruise, and landing phases resulting from the modifications to the current baseline configuration. Using a variety of aerodynamic theories, new aircraft lift curves and drag polars were developed. These new aerodynamic models were then used in the computer simulation to determine the new aircraft performance during the various phases of flight.

Based on a computational performance evaluation of new wing designs for the T-38 aircraft, the configuration with the increased wing area (S-1) should be chosen.

The S-1 configuration increases the baseline wing area from the current 170.0 square feet to 183.7 square feet. This is accomplished by increasing the span by one foot causing the root chord to increase by five inches and the tip chord by one inch. The aspect ratio remained constant at 3.75.

With a weight gain of only approximately 138 pounds, the operational envelope of the aircraft can be significantly increased. A 10 knot improvement in SETOS and a 7.5% reduction in landing distance will allow continued operation of the aircraft in the most demanding environmental conditions. Using advanced composites on other parts of the aircraft may help to offset this modest weight gain.

Wing areas larger than S-1, while providing continued gains to SETOS and landing distance, begin to add significant weight to this small training aircraft. In addition, the SETOS gains are much larger than needed.

Due to the fact that this wing is not much larger than the current wing (only about 5 inches at the root), fitting the wing to the current structure should not cause significant reengineering, although this will require further study beyond the scope the present work.

In conclusion, the original design analysis of almost fifty years ago was correct – the T-38 would have benefited greatly from a slightly larger wing. Then, as now, other factors prevented the production and design of a perfect aircraft. Overall though, the T-38 Talon has proven to be a resounding success as a supersonic trainer aircraft.

REFERENCES

REFERENCES

1. T-38 Talon, http://en.wikipedia.org/wiki/T-38_Talon [retrieved 8 February 2007].
2. “U.S. Air Force Fact Sheet, T-38 Talon,” Air Education and Training Command, Public Affairs Office, Randolph AFB, Texas, January 2006.
3. Kang, T.. *T-38C Block 5 Avionics Upgrade Program (AUP)*, FRR-06-05, Air Force Flight Test Center, Edwards AFB, California, August 2006.
4. Woolf, R. *T-38C Aircraft Performance Evaluation*, AFFTC-TR-03-18, Air Force Flight Test Center, Edwards AFB, California, September 2004.
5. Hayes B., Woo, W., and Guadagnini F., “Flight Manual Performance USAF Model T-38A Trainer Airplane with Two J85-GE-5 Engines,” Norair, Northrop Corporation, Hawthorne, California, December 1960.
6. Olson, W. and Nesst, D., “Digital Performance Simulation (DPS) Computer Program Users Guide”. Flight Dynamics Division, Air Force Flight Test Center, Edwards AFB, California, January 2006.
7. U.S. Standard Atmosphere, 1976, Joint Report of the National Oceanic and Atmospheric Administration (NOAA), National Aeronautics and Space Administration (NASA), and the United States Air Force, NOAA-S/T 76-1562, U.S. Government Printing Office, Washington, D.C., October 1976.
8. Raymer, D. P., *Aircraft Design: A Conceptual Approach*, AIAA Education Series, Second Printing, AIAA, Washington DC, 1989.
9. Flight Manual, USAF Series T-38A and AT-38B Aircraft, T.O. 1T-38A-1, August 2005.
10. Flight Manual, USAF Series T-38C, T.O. 1T-38C-1, April 2001, change 9, May 2006.
11. Abbott I. H. and von Doenhoff, A. E. *Theory of Wing Sections*, Dover Publications, Inc. New York, 1959.
12. Shevell, R. S. *Fundamentals of Flight*, Prentice-Hall, Inc. New Jersey, 1989.
13. Keenan, J. A. and Kuhlman, J. M. “Winglet Effectiveness on Low Aspect Ratio Wings at Supersonic Mach Numbers.” AIAA-91-3305-CP. AIAA, 1991.

APPENDICES

APPENDIX A

DPS Lift and Drag Data Files (Clean Configuration)

Lift Curve (Clean Configuration)

CLALFA 2 2 ALFA = f(AMIC,CL) 20JAN03
2 1 1 1
AMIC ND 27
0.000 0.400 0.500 0.600 0.650 0.700 0.750 0.800 0.825
0.850 0.875 0.900 0.910 0.920 0.930 0.940 0.950 0.960
0.980 1.000 1.020 1.050 1.100 1.150 1.200 1.250 1.600
CL ND 16
0.00 0.10 0.20 0.30 0.40 0.50 0.55 0.60
0.65 0.70 0.75 0.80 0.85 0.90 0.95 1.00
ALFA DEG
-0.03250 1.44679 2.92608 4.40537 5.88466 7.36395 8.10359 8.84324 9.80000
11.00000 12.35000 15.30000 20.30000 25.30000 30.00000 35.00000

-0.03250 1.44679 2.92608 4.40537 5.88466 7.36395 8.10359 8.84324 9.80000
11.00000 12.35000 15.30000 20.30000 25.30000 30.00000 35.00000

-0.06930 1.37370 2.81670 4.25970 5.70271 7.14571 7.86721 8.58871 9.60000
10.80000 12.35000 15.30000 20.30000 25.30000 30.00000 35.00000

-0.10360 1.29598 2.69556 4.09514 5.49472 6.89430 7.59409 8.29388 9.40000
10.70000 12.30000 14.10000 16.40000 19.40000 23.00000 26.00000

-0.12010 1.25258 2.62527 3.99795 5.37063 6.74332 7.42966 8.11600 9.30000
10.60000 12.20000 14.20000 16.70000 19.60000 23.00000 27.00000

-0.13460 1.20463 2.54385 3.88308 5.22230 6.56153 7.23114 7.90076 9.10000
10.50000 12.20000 14.20000 16.80000 19.80000 23.00000 27.00000

-0.14760 1.15279 2.45318 3.75357 5.05396 6.35435 7.00455 7.65474 9.00000
10.40000 12.20000 14.30000 16.70000 19.50000 23.00000 26.00000

-0.15910 1.09876 2.35662 3.61448 4.87235 6.13021 6.75914 7.38807 8.70000
10.20000 12.20000 14.30000 16.60000 19.10000 21.60000 24.00000

-0.17100 1.06357 2.29814 3.53270 4.76727 6.00184 6.61912 7.23641 8.30000
9.90000 11.50000 14.10000 16.40000 18.50000 21.00000 23.00000

-0.18600 1.02188 2.22975 3.43763 4.64550 5.85338 6.45731 7.06125 8.00000
9.00000 10.90000 13.00000 15.50000 17.90000 20.00000 22.00000

Lift Curve (Clean Configuration) (con't)

-0.20500	0.97147	2.14794	3.32441	4.50088	5.67735	6.26559	6.85382	7.70000
8.50000	10.00000	11.80000	14.10000	16.50000	19.00000	21.00000		
-0.22600	0.91425	2.05450	3.19475	4.33500	5.47525	6.04538	6.61551	7.18563
8.00000	9.30000	10.80000	12.80000	14.80000	17.50000	20.00000		
-0.23600	0.88760	2.01119	3.13479	4.25838	5.38198	5.94378	6.50557	7.06737
7.62917	8.70000	9.80000	11.50000	13.80000	17.00000	20.00000		
-0.24530	0.85967	1.96464	3.06962	4.17459	5.27956	5.83205	6.38453	6.93702
7.48951	8.04199	8.80000	10.10000	12.40000	16.00000	20.00000		
-0.25650	0.82575	1.90800	2.99025	4.07250	5.15476	5.69588	6.23701	6.90000
7.60000	8.30000	8.90000	9.70000	10.40000	11.50000	13.00000		
-0.27250	0.80884	1.89018	2.97151	4.05285	5.13419	5.67486	6.21553	6.90000
7.50000	8.20000	8.80000	9.60000	10.40000	11.50000	13.00000		
-0.29570	0.80356	1.90283	3.00209	4.10135	5.20062	5.75025	6.50000	7.10000
7.80000	8.50000	9.20000	9.90000	10.80000	12.00000	13.00000		
-0.28000	0.81300	1.90700	3.00000	4.09400	5.18700	5.70000	6.30000	6.90000
7.60000	8.40000	9.20000	9.90000	10.90000	12.00000	13.00000		
-0.36000	0.79000	1.93900	3.08900	4.23800	5.38700	5.90000	6.40000	7.10000
7.70000	8.40000	9.10000	9.90000	10.60000	11.70000	13.00000		
-0.42000	0.70500	1.83000	2.95500	4.08000	5.20500	5.90000	6.40000	7.10000
7.70000	8.30000	9.00000	9.70000	10.50000	11.70000	13.00000		
-0.61000	0.62500	1.85900	3.09400	4.32800	5.56300	6.10000	6.60000	7.30000
8.00000	8.50000	9.20000	10.00000	10.70000	11.70000	13.00000		
-0.61000	0.61300	1.83600	3.05900	4.28300	5.50600	6.10000	6.80000	7.40000
8.10000	8.80000	9.50000	10.20000	11.00000	12.00000	13.00000		
-0.72000	0.65400	2.02900	3.40300	4.77800	6.15300	6.80000	7.50000	8.10000
8.80000	9.60000	10.20000	10.80000	11.50000	12.10000	13.00000		
-0.30000	0.90000	2.00000	3.20000	4.50000	5.80000	6.50000	7.10000	7.90000
8.50000	9.20000	10.00000	10.70000	11.60000	12.40000	13.40000		

Lift Curve (Clean Configuration) (concluded)

-0.50000 0.80000 2.00000 3.30000 4.60000 5.90000 6.60000 7.20000 7.90000
8.70000 9.40000 10.20000 11.00000 11.80000 12.60000 13.50000

-0.60000 0.80000 2.10000 3.70000 5.20000 6.70000 7.50000 8.20000 9.00000
9.80000 10.70000 11.60000 12.40000 13.30000 14.20000 15.30000

-1.30000 0.60000 2.50000 4.30000 6.20000 8.20000 9.10000 10.10000
11.10000 12.10000 13.10000 14.10000 15.10000 16.10000 17.10000 18.20000

Drag Curve (Clean Configuration)

CDINDUCE 2 2 TABLE-XXX CDINDU = f(AMIC,CL) 12SEP00

2 1 1 1										
AMIC	ND 16									
0.00	0.20	0.40	0.60	0.70	0.80	0.85	0.90	0.95		
1.00	1.05	1.10	1.20	1.30	1.40	1.60				
CL	ND 64									
0.000	0.020	0.040	0.060	0.080	0.100	0.120	0.140	0.160		
0.180	0.200	0.220	0.240	0.260	0.280	0.300	0.305	0.310		
0.315	0.320	0.325	0.330	0.335	0.340	0.345	0.350	0.355		
0.360	0.365	0.370	0.375	0.380	0.385	0.390	0.395	0.400		
0.405	0.410	0.415	0.420	0.425	0.430	0.435	0.440	0.445		
0.450	0.455	0.460	0.465	0.470	0.475	0.480	0.485	0.490		
0.495	0.500	0.550	0.600	0.650	0.700	0.750	0.800	0.850		
0.900										

CDINDU	ND									
0.00017	0.00003	0.00000	0.00007	0.00025	0.00053	0.00092	0.00141	0.00200		
0.00270	0.00350	0.00440	0.00541	0.00652	0.00774	0.00906	0.00941	0.00986		
0.01033	0.01081	0.01130	0.01181	0.01234	0.01288	0.01343	0.01400	0.01463		
0.01528	0.01595	0.01664	0.01735	0.01808	0.01883	0.01960	0.02039	0.02120		
0.02196	0.02273	0.02352	0.02433	0.02516	0.02600	0.02687	0.02775	0.02865		
0.02957	0.03050	0.03146	0.03244	0.03343	0.03445	0.03548	0.03654	0.03762		
0.03871	0.03983	0.05446	0.07202	0.09370	0.12016	0.15210	0.19026	0.23546		
0.28855										

0.00012	0.00001	0.00001	0.00012	0.00033	0.00064	0.00105	0.00157	0.00220		
0.00293	0.00376	0.00469	0.00573	0.00688	0.00813	0.00948	0.00983	0.01030		
0.01078	0.01127	0.01178	0.01230	0.01284	0.01339	0.01396	0.01454	0.01519		
0.01586	0.01654	0.01725	0.01797	0.01872	0.01948	0.02027	0.02108	0.02190		
0.02268	0.02347	0.02427	0.02510	0.02594	0.02680	0.02768	0.02858	0.02949		
0.03043	0.03138	0.03236	0.03335	0.03436	0.03540	0.03645	0.03752	0.03862		
0.03973	0.04087	0.05562	0.07337	0.09524	0.12189	0.15400	0.19234	0.23770		
0.29094										

0.00007	0.00000	0.00003	0.00017	0.00041	0.00075	0.00120	0.00175	0.00240		
0.00316	0.00403	0.00499	0.00607	0.00724	0.00852	0.00990	0.01026	0.01074		
0.01123	0.01174	0.01226	0.01280	0.01335	0.01391	0.01449	0.01509	0.01575		
0.01644	0.01714	0.01786	0.01860	0.01937	0.02015	0.02095	0.02177	0.02262		
0.02341	0.02421	0.02503	0.02587	0.02673	0.02761	0.02851	0.02942	0.03035		
0.03130	0.03228	0.03327	0.03428	0.03531	0.03636	0.03743	0.03852	0.03963		
0.04076	0.04192	0.05691	0.07484	0.09691	0.12376	0.15607	0.19460	0.24014		
0.29355										

Drag Curve (Clean Configuration) (con't)

0.00005 0.00000 0.00005 0.00021 0.00047 0.00083 0.00130 0.00187 0.00255
0.00333 0.00421 0.00520 0.00629 0.00749 0.00879 0.01019 0.01056 0.01093
0.01131 0.01185 0.01241 0.01299 0.01358 0.01419 0.01482 0.01546 0.01612
0.01679 0.01747 0.01818 0.01890 0.01965 0.02041 0.02119 0.02199 0.02282
0.02361 0.02443 0.02526 0.02611 0.02698 0.02787 0.02878 0.02971 0.03065
0.03162 0.03260 0.03361 0.03463 0.03568 0.03675 0.03783 0.03894 0.04007
0.04122 0.04239 0.05731 0.07529 0.09740 0.12428 0.15661 0.19516 0.24069
0.29408

0.00007 0.00000 0.00004 0.00018 0.00042 0.00077 0.00122 0.00178 0.00244
0.00320 0.00407 0.00505 0.00612 0.00730 0.00859 0.00997 0.01034 0.01071
0.01108 0.01147 0.01186 0.01225 0.01265 0.01306 0.01374 0.01444 0.01500
0.01558 0.01618 0.01679 0.01741 0.01805 0.01870 0.01937 0.02005 0.02075
0.02150 0.02227 0.02306 0.02386 0.02469 0.02553 0.02639 0.02727 0.02816
0.02908 0.03002 0.03098 0.03195 0.03295 0.03397 0.03500 0.03606 0.03714
0.03824 0.03936 0.05265 0.06906 0.08923 0.11373 0.14319 0.17828 0.21974
0.26832

0.00010 0.00001 0.00002 0.00012 0.00032 0.00063 0.00103 0.00153 0.00213
0.00283 0.00363 0.00452 0.00552 0.00662 0.00781 0.00911 0.00945 0.00979
0.01014 0.01050 0.01086 0.01123 0.01161 0.01199 0.01238 0.01278 0.01324
0.01372 0.01420 0.01470 0.01520 0.01572 0.01625 0.01679 0.01733 0.01789
0.01859 0.01931 0.02004 0.02079 0.02156 0.02235 0.02316 0.02399 0.02483
0.02570 0.02659 0.02749 0.02842 0.02937 0.03033 0.03132 0.03233 0.03337
0.03442 0.03549 0.04709 0.06199 0.08035 0.10271 0.12967 0.16184 0.19990
0.24457

0.00008 0.00001 0.00002 0.00013 0.00034 0.00065 0.00105 0.00155 0.00214
0.00283 0.00361 0.00449 0.00547 0.00654 0.00771 0.00898 0.00931 0.00964
0.00999 0.01034 0.01069 0.01105 0.01142 0.01179 0.01217 0.01256 0.01300
0.01346 0.01392 0.01440 0.01488 0.01537 0.01587 0.01638 0.01691 0.01744
0.01812 0.01883 0.01955 0.02028 0.02104 0.02182 0.02261 0.02342 0.02426
0.02511 0.02598 0.02687 0.02778 0.02872 0.02967 0.03064 0.03164 0.03265
0.03369 0.03475 0.04595 0.06048 0.07838 0.10018 0.12645 0.15781 0.19490
0.23843

Drag Curve (Clean Configuration) (con't)

0.00006 0.00000 0.00004 0.00018 0.00041 0.00074 0.00116 0.00169 0.00230
0.00301 0.00382 0.00473 0.00573 0.00683 0.00802 0.00931 0.00964 0.00999
0.01034 0.01069 0.01105 0.01142 0.01179 0.01217 0.01256 0.01295 0.01340
0.01386 0.01434 0.01482 0.01531 0.01581 0.01632 0.01684 0.01737 0.01791
0.01857 0.01924 0.01994 0.02064 0.02137 0.02211 0.02287 0.02364 0.02444
0.02525 0.02607 0.02692 0.02778 0.02866 0.02956 0.03048 0.03142 0.03238
0.03335 0.03434 0.04502 0.05857 0.07512 0.09512 0.11907 0.14750 0.18097
0.22007

0.00006 0.00000 0.00005 0.00019 0.00044 0.00078 0.00123 0.00177 0.00242
0.00316 0.00401 0.00495 0.00600 0.00714 0.00839 0.00973 0.01008 0.01044
0.01080 0.01118 0.01155 0.01194 0.01232 0.01272 0.01312 0.01353 0.01400
0.01448 0.01497 0.01547 0.01598 0.01650 0.01703 0.01756 0.01811 0.01867
0.01932 0.01997 0.02065 0.02133 0.02203 0.02275 0.02348 0.02423 0.02499
0.02577 0.02656 0.02737 0.02819 0.02903 0.02989 0.03076 0.03165 0.03255
0.03348 0.03442 0.04470 0.05746 0.07287 0.09133 0.11326 0.13910 0.16933
0.20447

0.00007 0.00000 0.00004 0.00019 0.00045 0.00083 0.00132 0.00192 0.00263
0.00345 0.00439 0.00543 0.00659 0.00786 0.00925 0.01074 0.01113 0.01153
0.01194 0.01235 0.01277 0.01319 0.01363 0.01407 0.01452 0.01497 0.01545
0.01595 0.01645 0.01695 0.01747 0.01800 0.01853 0.01907 0.01962 0.02018
0.02081 0.02145 0.02210 0.02276 0.02343 0.02412 0.02482 0.02553 0.02625
0.02698 0.02773 0.02849 0.02927 0.03005 0.03085 0.03166 0.03249 0.03332
0.03418 0.03504 0.04447 0.05574 0.06902 0.08454 0.10259 0.12346 0.14747
0.17495

0.00011 0.00001 0.00003 0.00018 0.00046 0.00086 0.00139 0.00204 0.00282
0.00372 0.00475 0.00591 0.00719 0.00860 0.01013 0.01179 0.01222 0.01266
0.01311 0.01357 0.01404 0.01451 0.01499 0.01548 0.01598 0.01648 0.01699
0.01751 0.01804 0.01858 0.01912 0.01967 0.02023 0.02080 0.02138 0.02196
0.02259 0.02324 0.02389 0.02456 0.02523 0.02592 0.02661 0.02732 0.02804
0.02876 0.02950 0.03025 0.03101 0.03178 0.03256 0.03335 0.03415 0.03496
0.03579 0.03662 0.04575 0.05634 0.06853 0.08247 0.09834 0.11635 0.13669
0.15959

Drag Curve (Clean Configuration) (con't)

0.00014 0.00001 0.00003 0.00018 0.00048 0.00092 0.00150 0.00222 0.00308
0.00409 0.00524 0.00652 0.00796 0.00953 0.01124 0.01310 0.01358 0.01408
0.01458 0.01509 0.01561 0.01614 0.01668 0.01723 0.01779 0.01835 0.01893
0.01951 0.02010 0.02070 0.02131 0.02193 0.02256 0.02319 0.02384 0.02449
0.02516 0.02583 0.02651 0.02720 0.02790 0.02860 0.02932 0.03004 0.03078
0.03152 0.03227 0.03303 0.03380 0.03458 0.03537 0.03616 0.03697 0.03778
0.03860 0.03943 0.04884 0.05935 0.07118 0.08444 0.09924 0.11569 0.13392
0.15407

0.00025 0.00004 0.00001 0.00018 0.00053 0.00106 0.00178 0.00269 0.00379
0.00507 0.00654 0.00819 0.01003 0.01206 0.01427 0.01667 0.01730 0.01794
0.01859 0.01926 0.01993 0.02062 0.02132 0.02203 0.02275 0.02349 0.02423
0.02499 0.02576 0.02654 0.02733 0.02814 0.02895 0.02978 0.03062 0.03147
0.03233 0.03320 0.03409 0.03499 0.03590 0.03682 0.03775 0.03869 0.03965
0.04061 0.04159 0.04258 0.04358 0.04460 0.04562 0.04666 0.04771 0.04877
0.04984 0.05092 0.06339 0.07730 0.09304 0.11078 0.13068 0.15293 0.17771
0.20523

0.00035 0.00006 0.00001 0.00018 0.00058 0.00121 0.00207 0.00315 0.00447
0.00601 0.00779 0.00979 0.01202 0.01448 0.01717 0.02008 0.02085 0.02163
0.02242 0.02323 0.02405 0.02489 0.02574 0.02661 0.02748 0.02838 0.02929
0.03021 0.03115 0.03210 0.03306 0.03404 0.03504 0.03604 0.03707 0.03810
0.03915 0.04022 0.04130 0.04239 0.04350 0.04462 0.04576 0.04691 0.04808
0.04926 0.05045 0.05166 0.05288 0.05412 0.05537 0.05664 0.05792 0.05921
0.06052 0.06184 0.07717 0.09430 0.11374 0.13571 0.16043 0.18813 0.21908
0.25354

0.00043 0.00008 0.00001 0.00020 0.00067 0.00141 0.00243 0.00371 0.00527
0.00710 0.00920 0.01157 0.01422 0.01714 0.02033 0.02379 0.02469 0.02562
0.02656 0.02752 0.02850 0.02949 0.03050 0.03152 0.03257 0.03363 0.03471
0.03580 0.03691 0.03804 0.03919 0.04035 0.04153 0.04273 0.04394 0.04517
0.04642 0.04769 0.04897 0.05027 0.05158 0.05291 0.05426 0.05563 0.05701
0.05842 0.05983 0.06127 0.06272 0.06419 0.06567 0.06718 0.06870 0.07023
0.07179 0.07336 0.09167 0.11203 0.13517 0.16132 0.19076 0.22378 0.26068
0.30180

Drag Curve (Clean Configuration) (concluded)

0.00042 0.00005 0.00004 0.00039 0.00110 0.00216 0.00359 0.00537 0.00751
0.01001 0.01287 0.01609 0.01966 0.02360 0.02789 0.03254 0.03376 0.03500
0.03626 0.03755 0.03886 0.04019 0.04154 0.04291 0.04431 0.04573 0.04717
0.04864 0.05013 0.05164 0.05317 0.05472 0.05630 0.05790 0.05952 0.06117
0.06283 0.06452 0.06623 0.06797 0.06972 0.07150 0.07330 0.07513 0.07697
0.07884 0.08073 0.08264 0.08458 0.08654 0.08852 0.09052 0.09254 0.09459
0.09666 0.09875 0.12277 0.14945 0.17958 0.21344 0.25134 0.29360 0.34057
0.39263

APPENDIX B

DPS Lift and Drag Data Files (Flaps 60% Configuration)

Lift Curve (Flaps 60% Configuration)

```
CLOGE60G  2  2  TABLE-XXX  ALFA=f(CL) 20Dec2005
  1  1  1  1
CL        ND        6
0.0200  0.3000  0.7800  0.8500  0.9150  0.9700
ALFA     ND
-5.000  0.0000  7.5000  9.0000  11.000  22.000
```

Drag Curve (Flaps 60% Configuration)

```
CDOGE60G  2  2  TABLE-XXX  CD = f(CL) 21Dec2005
  1  1  1  1
CL        ND        27
0.00000  0.05000  0.10000  0.15000  0.20000  0.25000
0.30000  0.32500  0.35000  0.37500  0.40000  0.42500
0.45000  0.47500  0.50000  0.55000  0.60000  0.62500
0.65000  0.70000  0.75000  0.80000  0.85000  0.90700
0.92100  0.92700  0.95500
CDG      ND
0.04656  0.04266  0.03987  0.03820  0.03764  0.03820
0.03987  0.04112  0.04266  0.04447  0.04656  0.04893
0.05158  0.05450  0.05771  0.06496  0.07332  0.07955
0.08616  0.10050  0.11636  0.13372  0.15800  0.20000
0.21600  0.24000  0.40000
```

APPENDIX C

DPS Input files

SETOS Level acceleration:

The DPS input file can be seen in Figure C-1.

```
$DPS H=4000.0, XENG=2, PCODE=45., INZ=1, ANZ=1., WT=13000.$  
$DPS AM=0.10, DMI=0.02, AMF=0.5, MANUVR=2, MINS=1, MISS=0$  
$DPS IPRINT(3)=1, DELTAT=30.$  
$DPS XIN(1)=18400., XIN(2)=20.0, XIN(3)=1, XIN(4)=60, XIN(6)=0$  
$DPS XIN(10)=0, XIN(11)=-115, XIN(12)=2$  
$DPS XIN(20)=183.7319871$  
T-38C SE Level Accel  
$DPS IEND=1$
```

Figure C-1. Example of DPS input file for SETOS level acceleration.

SETOS Climb:

The DPS input file can be seen in Figure C-2.

```
$DPS H=3500.0, DHI=100, HF=4500.0, XENG=2, PCODE=45., WT=13000.$  
$DPS AMC=0.0, VCCK=161.034, MANUVR=1, MINS=1, MISS=0$  
$DPS IPRINT(3)=1, DELTAT=30.$  
$DPS XIN(1)=18400., XIN(2)=20.0, XIN(3)=1, XIN(4)=60, XIN(6)=0$  
$DPS XIN(10)=0, XIN(11)=-115, XIN(12)=2$  
T-38C Sawtooth Climb  
$DPS IEND=1$
```

Figure C-2. Example of DPS input file for SETOS climb.

Maximum Range:

The DPS input file can be seen in Figure C-3.

```
$DPS AM=0.6, DMI=0.001, AMF=0.9, MANUVR=7, MINS=1, MISS=0$  
$DPS IPRINT(3)=1, DELTAT=0.$  
$DPS XIN(1)=18400., XIN(2)=20.0, XIN(3)=1, XIN(4)=0, XIN(6)=0, XIN(12)=2$  
T-38C Max Range  
$DPS IEND=1$
```

Figure C-3. Example of DPS input file for maximum range.

DPS Input files (con't)

Maximum Speed:

The DPS input file can be seen in Figure C-4.

```
$DPS H=0.0,DHI=1000,HF=45000.0,XENG=2,PCODEM=44,WT=10000.$  
$DPS AM=0.7,MANUVR=11,MINS=1,MISS=0$  
$DPS IPRINT(3)=1,DELTAT=0.$  
$DPS XIN(1)=18400.,XIN(2)=20.0,XIN(3)=1,XIN(4)=0,XIN(6)=0,XIN(12)=2$  
T-38C Max Speed  
$DPS IEND=1$
```

Figure C-4. Example of DPS input file for maximum speed profile.

DPS Input Variable List

- XIN (1) = Fuel Heating Value (BTU/lbm)
XIN (2) = Location of CG in %MAC
XIN (3) = Configuration: (1 = OGE, 2: Not used, 3 = IGE)
XIN (4) = Flap configuration: (0 = clean, 60 = 60% flaps, 100 = 100% flaps)
XIN (5) = Travel Pod (IACONFG) flag.
 0 = default (pod not installed)
 1 = travel pod installed
XIN (6) = Landing gear configuration
 (0=retracted, 1=extended, doors closed, 2=extended, doors open)
XIN (7) = Speed brake configuration: (0 = retracted, 1 = extended)
XIN (8) and XIN (9) = Not used
XIN(10) = Part power mode switch (PCODE must be set to 55):
 0 = PLA is power setting parameter,
 1 = engine RPM (%) is power setting parameter
XIN(11) = User-specified power setting parameter
 (either PLA or engine RPM (%) depending on the value of XIN(10))
XIN(12) = IENGMOD parameter: 0 = Default (uses GE model);
 1 = Baseline;
 2 = Fullup (AFFTC eng model);
 3 = Ejector-only.
XIN(13) and XIN(14) = Not used
XIN(15) = Max normal load factor (ANZMAX)
XIN(16), XIN(17), and XIN(18) = Not used
XIN(19) = Turns on/off curve file opening messages (0 = OFF, 1 = ON)
XIN(20) = Wing Reference Area (square feet). Reference value is 170.0

Notes:

XIN(10)=0 for 80% power

XIN(11):

- 94 = 5M Windmill/MIL
- 115 = 5M windmill/MAX
- 120 = 5R windmill/MAX PCODE = 75
- 10 = IDLE PCODE = 1
- 80 = 80% part power PCODE = 55
- 90 = 5R MIL PCODE = 55
- 94 = 5M MIL PCODE = 22
- 95 = Min A/B PCODE = 66
- 115 = 5M MAX PCODE = 44
- 120 = 5R MAX PCODE = 77

VITA

Major John M. Kanuch is an F-16 Test Pilot and has served in the United States Air Force for the past 14 years. He currently lives with his wife and son in Fort Worth, Texas.